



# Epigenetic, genetic and maternal effects enable stable centromere inheritance

Arunika Das<sup>1,2,3,4</sup>, Aiko Iwata-Otsubo<sup>2,5</sup>, Aspasia Destouni<sup>1,6</sup>, Jennine M. Dawicki-McKenna<sup>1</sup>, Katelyn G. Boese<sup>2</sup>, Ben E. Black<sup>1,3,4</sup> and Michael A. Lampson<sup>1,2,3</sup>

**Centromeres are defined epigenetically by the histone H3 variant CENP-A. The propagation cycle by which pre-existing CENP-A nucleosomes serve as templates for nascent assembly predicts the epigenetic memory of weakened centromeres. Using a mouse model with reduced levels of CENP-A nucleosomes, we find that an embryonic plastic phase precedes epigenetic memory through development. During this phase, nascent CENP-A nucleosome assembly depends on the maternal *Cenpa* genotype rather than the pre-existing template. Weakened centromeres are thus limited to a single generation, and parental epigenetic differences are eliminated by equal assembly on maternal and paternal centromeres. These differences persist, however, when the underlying DNA of parental centromeres differs in repeat abundance, as assembly during the plastic phase also depends on sufficient repetitive centromere DNA. With contributions of centromere DNA and the *Cenpa* maternal effect, we propose that centromere inheritance naturally minimizes fitness costs associated with weakened centromeres or epigenetic differences between parents.**

Centromeres are essential for faithful mitotic and meiotic segregation of chromosomes as vehicles for genetic inheritance<sup>1</sup>. There is strong evidence for genetic contributions from typically highly repetitive centromere DNA in centromere function<sup>2</sup> and competition in female meiotic drive<sup>3–6</sup>. However, mammalian chromosomes lacking typical centromere DNA reveal the essential epigenetic component<sup>7–10</sup> provided by nucleosomes containing the histone H3 variant, CENP-A<sup>11</sup>. In somatic cells, centromere chromatin is maintained by an epigenetic propagation cycle in which pre-existing CENP-A nucleosomes dictate local nascent CENP-A chromatin assembly<sup>12–16</sup>, suggesting epigenetic memory of the number of CENP-A nucleosomes. In the germline, such memory implies that any reduction in CENP-A chromatin would persist to the next generation. Differences between maternal and paternal centromeres would also persist, leading to asymmetries associated with embryonic aneuploidy and even elimination of one parental genome in plants<sup>17,18</sup> and with biased segregation of paired homologous chromosomes in meiosis<sup>4,5</sup>. Epigenetic memory from one generation to the next through the germline has not been tested in mammals, and the results in other model systems are conflicting. Lowering the levels of a CENP-A transgene in fruit fly sperm led to lower levels of CENP-A in some chromosomes of offspring<sup>19</sup>, consistent with epigenetic memory. In worms, however, centromere identity is thought to be independent of CENP-A nucleosomes inherited from the previous generation<sup>20</sup>. Thus, whether or not there is memory of the state of centromeric chromatin between generations remains an open question.

## Results

### Weakened centromeres persist in the male germline and soma.

To test for epigenetic memory of weakened centromeres with reduced CENP-A chromatin in mammals, we generated heterozygous (H) *Cenpa*<sup>+/-</sup> mice (Methods). CENP-A chromatin is reduced

to  $43.0 \pm 0.019\%$ ,  $48.6 \pm 0.003\%$  and  $53.8 \pm 0.004\%$  (mean  $\pm$  s.e.m.) of control levels in the soma, male gametes and female gametes, respectively, from these animals (Fig. 1a–c and Extended Data Fig. 1, P<sub>0</sub> generation). This model system allows us to test two predictions of epigenetic memory between generations. First, weakened centromeres inherited from the gametes should persist in genetically wild-type (WT) animals. In a cross between two *Cenpa*<sup>+/-</sup> parents (H  $\times$  H), *Cenpa*<sup>+/+</sup> progeny should maintain reduced CENP-A chromatin (Fig. 1b, F1 generation). Second, memory should be centromere-autonomous, with each centromere remembering its own level, so that inherited differences persist through development. In a cross between a *Cenpa*<sup>+/+</sup> mother and a *Cenpa*<sup>+/-</sup> father (WT♀  $\times$  H♂), *Cenpa*<sup>+/+</sup> progeny should maintain a large epigenetic difference between the maternal and paternal centromeres.

For the first prediction, we find reduced CENP-A levels ( $72.7 \pm 0.005\%$ ) at centromeres in the male germline of *Cenpa*<sup>+/-</sup> progeny of *Cenpa*<sup>+/-</sup> parents, relative to controls with WT parents (Fig. 1c,d and Extended Data Fig. 2). Thus, weakened centromeres persists through development of the male germline in the next generation, consistent with epigenetic memory, although the partial recovery suggests that the memory is incomplete. In contrast, the female germline nearly completely recovers centromere chromatin ( $94.7 \pm 0.008\%$  of controls with WT parents), indicating loss of epigenetic memory in one generation (Fig. 1c,d and Extended Data Fig. 3a). This unexpected dichotomy is underscored by analysis of male and female littermates showing differential recovery of centromere chromatin in their germlines (Extended Data Fig. 3b). Our results raise the question of whether weakened centromeres persist in somatic tissues. Using bone marrow as a representative tissue, we find reduced CENP-A levels in both male and female soma, like the male germline ( $69.7 \pm 0.012\%$ , Fig. 2 and Extended Data Fig. 3a). These results are consistent with epigenetic centromere

<sup>1</sup>Department of Biochemistry and Biophysics; Perelman School of Medicine, University of Pennsylvania, Philadelphia, PA, USA. <sup>2</sup>Department of Biology, University of Pennsylvania, Philadelphia, PA, USA. <sup>3</sup>Penn Center for Genome Integrity, University of Pennsylvania, Philadelphia, PA, USA. <sup>4</sup>Epigenetics Institute, University of Pennsylvania, Philadelphia, PA, USA. <sup>5</sup>Present address: Department of Medical and Molecular Genetics, Indiana University School of Medicine, Indianapolis, IN, USA. <sup>6</sup>Present address: Laboratory of Cytogenetics and Molecular Genetics, Faculty of Medicine, University of Thessaly, Larissa, Greece. e-mail: [blackbe@pennteam.upenn.edu](mailto:blackbe@pennteam.upenn.edu); [lampson@sas.upenn.edu](mailto:lampson@sas.upenn.edu)

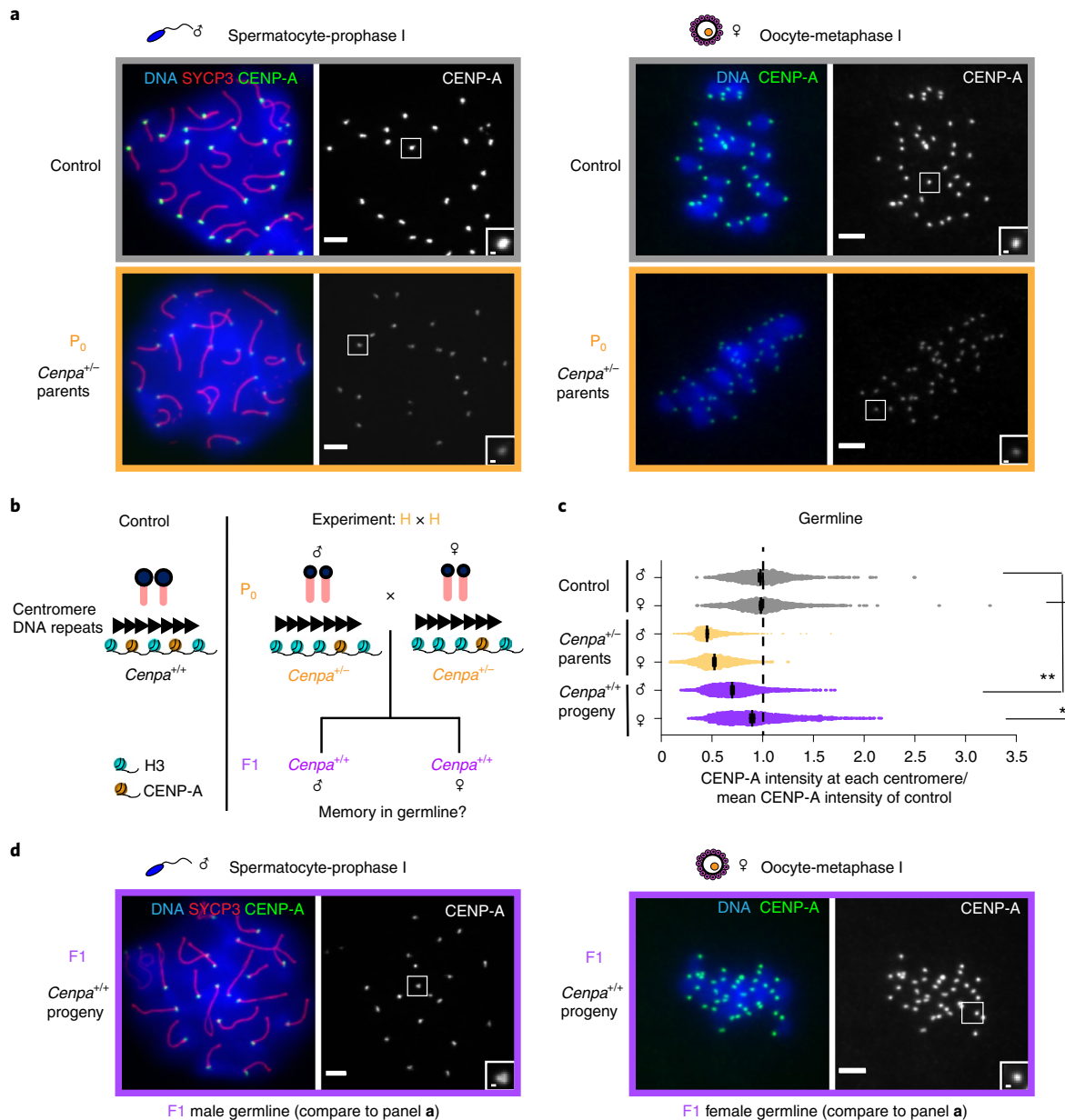


**Fig. 1 | Evidence for epigenetic centromere memory through mouse reproduction. a**, Spermatocytes at prophase I and oocytes at metaphase I for the  $P_0$  generation compared with control. Each of the CENP-A foci represents four centromeres in spermatocytes (a pair of homologous chromosomes, each with two sisters) or two sister centromeres in oocytes. SYCP3, a synaptonemal complex element, marks prophase I spermatocytes. **b**, Mating scheme to test memory in the F1 generation. **c**, Quantification of CENP-A foci intensities in control (grey),  $P_0$  (yellow) and F1 (purple) generations in germline (**a** and **d**).  $N = 1,576, 1,608, 1,722, 1,412, 1,836$  and  $1,473$  centromeres (top to bottom). \*\* $P < 0.0001$ , \* $P < 0.05$ , Mann-Whitney U test (two-tailed). Error bars: median  $\pm$  95% CI. See also Supplementary Table 1. **d**, Spermatocyte and oocyte at prophase I (left) and metaphase I (right), respectively (F1 generation). Scale bars,  $5 \mu\text{m}$  (main panel) and  $1 \mu\text{m}$  (inset).

memory between generations and through mouse development, but the female germline recovers normal CENP-A chromatin levels.

**Zygotic centromere differences are not maintained in adults.** Before testing the second prediction (Fig. 3a), we noted that zygotes from WT × WT crosses exhibit lower CENP-A levels on paternal centromeres identified by the absence of H3K9me3<sup>21–23</sup> (paternal/maternal ratio = 0.5; Fig. 3b,c). Mammalian CENP-A nucleosomes are retained robustly in sperm<sup>24–26</sup> relative to canonical nucleosomes, which are largely replaced by protamines, and indeed we find no measurable loss of CENP-A nucleosomes during the histone-to-protamine exchange in spermiogenesis (Fig. 3d,e

and Extended Data Fig. 4). The difference between maternal and paternal centromeres in the zygote could reflect either some loss of CENP-A nucleosomes during the protamine-to-histone exchange in the zygote and/or excess loading in the oocyte consistent with the recovery observed in the  $Cenpa^{+/+}$  progeny of  $Cenpa^{+/-}$  parents (Fig. 1). As we anticipated, the difference between maternal and paternal centromeres is enhanced (ratio = 0.4) in F1 zygotes from the WT♀ × H♂ cross compared to the WT × WT cross (Fig. 3b,c). This result does not depend on the zygotic genotype, because the zygotic genome is not transcribed at this stage. To determine whether this zygotic difference is maintained in adults, as predicted by centromere-autonomous epigenetic memory<sup>12,15</sup>,

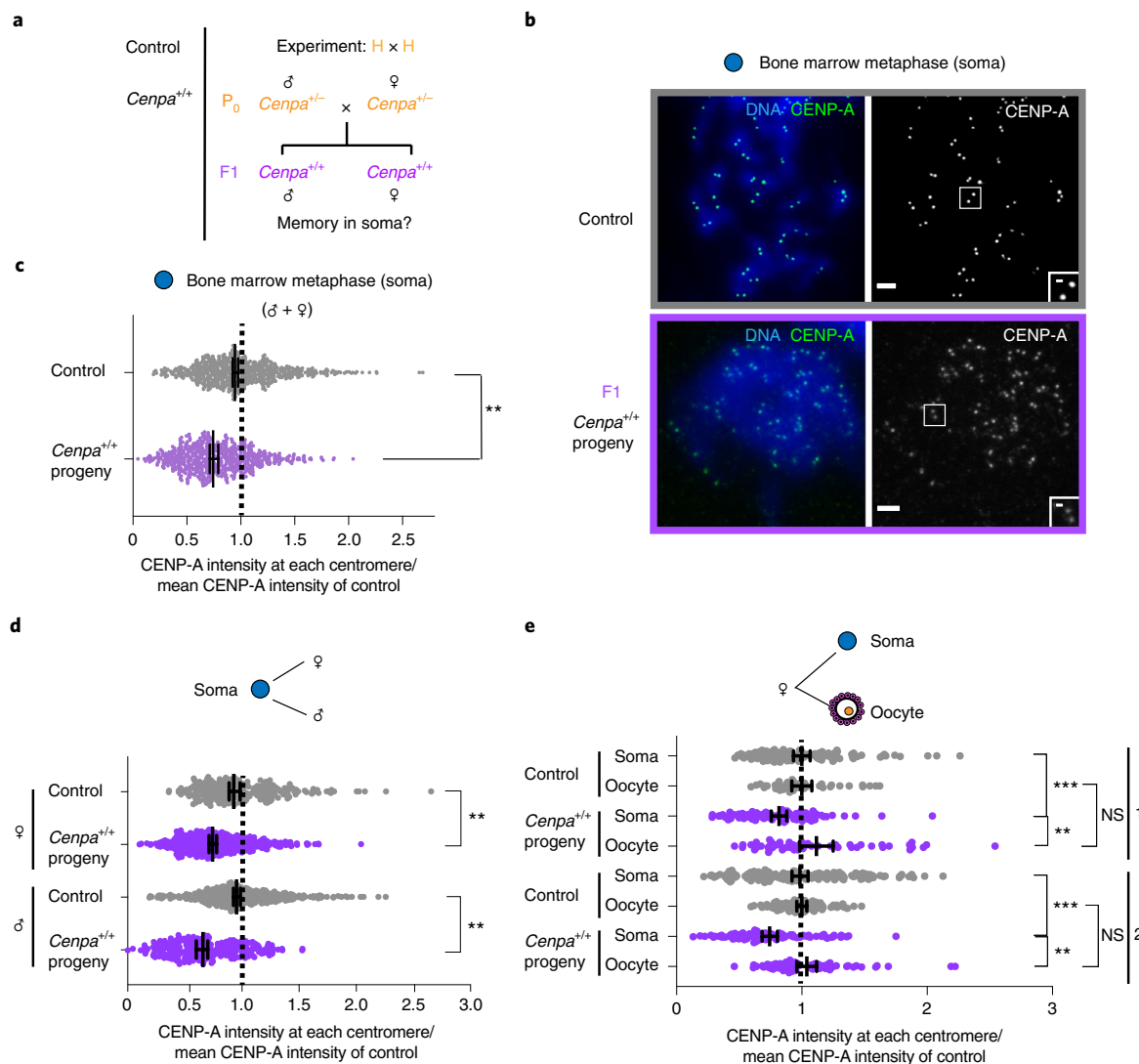


**Fig. 2 | Male and female soma show reduced CENP-A compared to oocytes.** **a**, Mating scheme to test memory in soma in the F1 generation. **b**, Bone marrow metaphase spreads (control and F1 generation) are representative of both male and females: each pair of CENP-A foci represents sister centromeres in mitosis. **c**, Quantification of CENP-A foci intensities in control (grey) and F1 (purple) generations in male and female soma combined.  $N = 642$  and  $684$  centromeres (top to bottom).  $**P < 0.0001$ , Mann-Whitney U test (two-tailed). **d**, Pooled male and female CENP-A intensities from **c**, replotted with male and female separated to show that both contain weakened centromeres.  $N = 251, 433, 390$  and  $251$  centromeres (top to bottom).  $**P < 0.0001$ . **e**, Quantification of CENP-A foci intensities showing weakened centromeres in the soma compared with oocytes from the same female. Two independent experiments (1 and 2) are shown, each comparing a single F1 animal (from H  $\times$  H cross) to controls.  $N = 112, 44, 94, 51, 169, 89, 98$  and  $68$  centromeres (top to bottom).  $***P < 0.001$ ,  $**P < 0.01$ , Mann-Whitney U test (two-tailed). NS, not significant. Error bars: median  $\pm$  95% CI. Scale bars,  $5 \mu\text{m}$  (main panel) and  $1 \mu\text{m}$  (inset).

we analysed meiotic bivalents containing one centromere inherited from each parent. In both the female and male germlines, we find that the ratio between the centromeres of paired homologous chromosomes is indistinguishable from controls (Fig. 3f,g), indicating that initial zygotic differences are not maintained. These results from the WT $\text{Q} \times \text{H}\delta$  cross are inconsistent with epigenetic centromere memory, in contrast to the results from the H  $\times$  H cross.

**Centromere strength depends on the maternal *Cenpa* genotype.** The conflicting results from our H  $\times$  H and WT $\text{Q} \times \text{H}\delta$  crosses suggest that the weakened centromere state in the progeny might reflect a reduced maternal pool of *Cenpa* gene products, rather than the number of CENP-A nucleosomes inherited in the gametes. To investigate this possibility, we compared reciprocal crosses in which either parent is heterozygous and the other is WT

(Fig. 4a) to our original H  $\times$  H cross. We find that the maternal genotype is key: if the mother is heterozygous, the weakened centromere state persists in the male germline of the F1 progeny, regardless of whether the father has weakened centromeres ( $72.7 \pm 0.005\%$  versus  $78.4 \pm 0.008\%$ , both relative to control; Fig. 4b–d). Conversely, if the mother is WT, then weakened paternal centromeres completely recover in the male germline of the F1 progeny ( $104.1 \pm 0.024\%$  relative to control; Fig. 4c,d). Consistent with this result, we find that the maternal but not the paternal *Cenpa* $^{+/-}$  heterozygous genotype has functional consequences for reproductive fitness, with reduced litter size only when the mother is heterozygous (Fig. 4e).

Given that the persistence of weakened centromeres depends on the maternal genotype, we predicted that an epigenetically weakened centromere state in a WT genotype can only last for a single generation. To test this prediction, we crossed *Cenpa* $^{+/-}$

F1 males and females with weak centromeres, obtained from the H×H cross, to generate F2 animals (Fig. 5a). We find, in line with our expectations, that centromere chromatin almost completely recovers to control levels in the male germline of F2 animals ( $93.9 \pm 0.01\%$ ; Fig. 5b,c).

The importance of the maternal genotype suggests that centromere strength is determined during the early embryonic cell cycles, before zygotic genome activation (ZGA), when nascent centromere chromatin assembly would depend on maternally provided protein and/or a pool of messenger RNA (mRNA) rather than the zygotic genotype. Indeed, our experimental results are consistent with simple modelling of this process in the first two embryonic cell cycles, based on three assumptions (Extended Data Fig. 5). First, new assembly is reduced by 50% in early embryos with heterozygous mothers due to the reduced maternal contribution. Second, assembly is equal on maternal and paternal centromeres. Third, weakened centromeres persist by epigenetic memory after the first two cell cycles, even after activation of a WT zygotic genome. This model captures both partial restoration of weakened centromere chromatin (Figs. 1c and 4c) and equalization of the initial differences between the maternal and paternal centromeres (Fig. 3). At the molecular level, mouse oocytes do not harbour a large pool of CENP-A protein<sup>27</sup>, although a small pool may exist and suffice. However, we find that the *Cenpa* 3' untranslated region (UTR) has hallmark sequences of a dormant maternal mRNA (Extended Data Fig. 6): a class of transcripts stored in a full-grown oocyte and translated in the embryo to support cellular functions prior to ZGA<sup>28</sup>. Previous microarray data<sup>29</sup> show an increase in *Cenpa* transcripts containing long poly(A) tails when oocytes transition to one-cell embryo, consistent with recruitment of dormant maternal mRNAs after fertilization. Thus, we define *Cenpa* as a maternal effect gene, as the maternal contribution determines centromere strength.

**Centromeres equalize in early embryogenesis.** To test our model prediction that centromeres equalize within the early embryonic cell cycles (Extended Data Fig. 5), we examined four-cell embryos from the WT×WT (control) cross and the WT♀×H♂ cross, which maximizes the difference between maternal and paternal centromeres (Fig. 3c). By this stage, paternal chromosomes have gained H3K9me3<sup>21</sup> (Extended Data Fig. 7), and other major chromatin rearrangements have occurred, including broad decoration of chromosomes with nucleosomes harbouring the histone H3.3 variant<sup>30</sup>. In the absence of a cytological marker for paternal versus maternal chromosomes at the four-cell stage, we analysed the distributions of CENP-A intensities to determine whether or not two populations of centromeres (low and high CENP-A levels) persist. In one-cell zygotes, we find bimodal distributions of the pooled maternal and paternal centromeres (Fig. 6a and Extended Data Fig. 8), consistent with our previous analysis (Fig. 3c). Bimodality is lost by the four-cell stage, consistent with our model prediction (Extended Data Fig. 5), with the resulting unimodal distributions similar to those obtained

from spermatocyte centromeres of F1 adult animals (Fig. 6a), which are expected to be unimodal. These results indicate that the first two cell cycles after fertilization represent a phase of plasticity when CENP-A nucleosomes rapidly equalize between parental centromeres to levels determined by the maternal genotype.

**A genetic pathway equalizes centromeres in embryos.** We next considered how nascent centromere chromatin assembly could be equal on maternal and paternal centromeres, as in our model (Extended Data Fig. 5), despite initial differences in centromere chromatin. Epigenetic memory depends on existing CENP-A nucleosomes directing nascent assembly by binding CENP-C, the centromere component that recruits downstream assembly factors, including the Mis18 complex and the dedicated CENP-A chaperone, HJURP<sup>12,14,31–35</sup>. However, we suspected that a genetic contribution might be more important than the epigenetic pathway during the early embryonic cell cycles. The centromeres in all the animals used in our crosses (Figs. 1–5 and 6a) have an identical genetic makeup, with an excess of minor satellite sequences present at each centromere relative to the number of CENP-A nucleosomes<sup>4</sup>. Minor satellite monomer units (120bp) house a preferred assembly site for CENP-A nucleosomes<sup>4</sup>, as well as the binding element (CENP-B box) for the sequence-specific DNA-binding protein, CENP-B<sup>36</sup>. Given that CENP-B contributes to CENP-C recruitment to centromeres<sup>37,38</sup>, we predicted that CENP-C might be sensitive to minor satellite DNA rather than to epigenetic differences between paternal and maternal centromeres in the zygote. Indeed, in zygotes from the WT×WT cross, CENP-C is only slightly different between the paternal and maternal centromeres (paternal/maternal ratio =  $0.80 \pm 0.04$  for CENP-C versus  $0.51 \pm 0.04$  for CENP-A; Fig. 6b,f). Furthermore, increasing the epigenetic differences in the WT♀×H♂ cross has little effect on CENP-C (paternal/maternal ratio =  $0.73 \pm 0.04$  for CENP-C versus  $0.38 \pm 0.03$  for CENP-A; Fig. 6c,f). These findings suggest that the genetic pathway directs CENP-C recruitment and centromere chromatin assembly in the early embryo, leading to epigenetic equalization when centromeres are genetically identical.

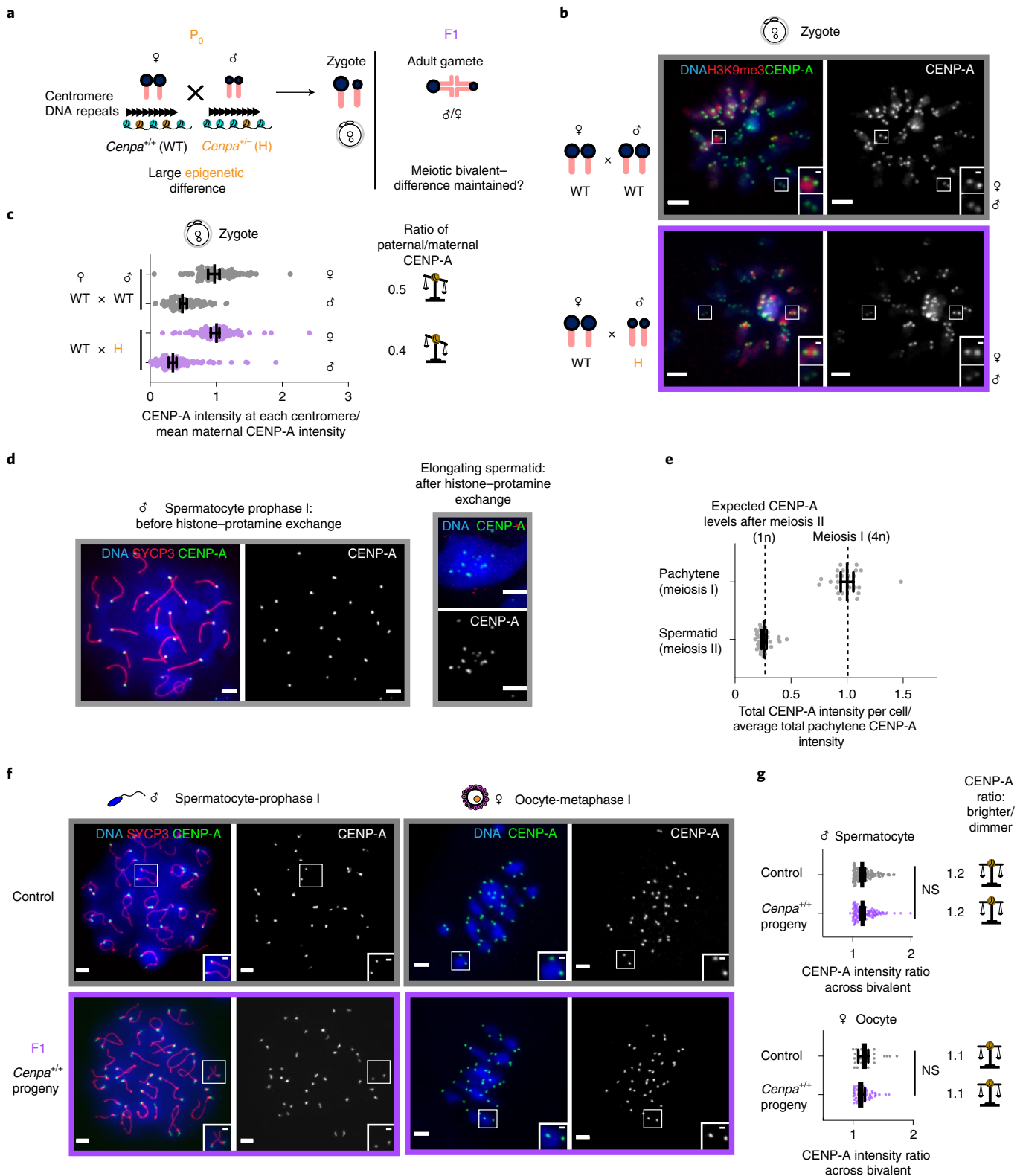
We took two approaches to test this hypothesis. First, we took advantage of natural variation between mouse strains to restrict the genetic contribution by reducing the number of minor satellite repeats. The CHPO strain harbours tiny centromere arrays (six-fold to tenfold smaller than C57BL/6J) that restrict both CENP-A nucleosome assembly and CENP-B boxes<sup>4</sup>. Owing to these genetic differences, we predicted larger CENP-C differences between paternal and maternal centromeres in zygotes from a WT♀×CHPO♂ cross compared to our previous WT×WT or WT♀×H♂ crosses. Indeed, the CENP-C ratio is significantly reduced ( $0.58 \pm 0.03$ ) in WT♀×CHPO♂ zygotes relative to the previous crosses, indicating an increase in CENP-C difference between the two parents (Fig. 6d,f). Moreover, this initial difference in CENP-A nucleosomes and CENP-C between maternal and paternal centromeres in

**Fig. 3 | Epigenetic differences between parental centromeres are not maintained.** **a**, Mating scheme to create epigenetic differences between maternal and paternal centromeres in F1. **b**, Zygotes (one-cell embryos) from WT×WT (control) and WT♀×H♂ crosses. Each pair of CENP-A foci represents sister centromeres in mitosis. Insets show 1.5× magnified maternal and paternal centromeres distinguished by H3K9me3. **c**, Quantifications of maternal and paternal CENP-A intensities are shown in zygotes combined from two independent experiments with ratios designated for each cross;  $N = 89, 90, 145$  and 143 centromeres (top to bottom). The balance symbols indicate the extent of epigenetic differences between parental centromeres. **d**, Representative images of spermatocyte pachytene (prophase of meiosis I, 4n) and an elongating spermatid (after completing meiosis II and histone-protamine exchange<sup>50,51</sup>, 1n) from control (*Cenpa*<sup>+/+</sup>) animals. **e**, Quantification of total CENP-A levels per cell;  $N = 26$  spermatocytes or 35 spermatids. The observed reduction to 25% in spermatids (1n) compared with prophase I spermatocytes (4n) is expected if there is no loss during the histone-protamine exchange. **f**, Diplotene spermatocyte spreads and metaphase I oocytes in F1. During diplotene, centromeres of paired homologous chromosomes (marked with SYCP3 in red) can be resolved. Each inset shows a pair of homologous chromosomes (bivalent), and each of the CENP-A foci represents two sister centromeres. **g**, Quantification of the ratio of CENP-A foci intensities across a meiotic bivalent (brighter/dimmer) in male and female gametes from **d**;  $N = 122, 124, 30$  and 56 bivalents (top to bottom). NS,  $P > 0.05$ ; Mann-Whitney U test (two-tailed). Error bars, median ± 95% CI. Scale bars, 5 μm (main panel) and 1 μm (inset).

WT♀ × CHPO♂ zygotes is maintained in the adult, leading to asymmetric bivalents that show biased segregation in meiosis<sup>4</sup>. These results indicate that nascent assembly of CENP-A nucleosomes depends on the genetic pathway during the plastic phase, such that centromere chromatin equalizes only when genetically identical.

As a second approach, we eliminated the CENP-B-dependent genetic pathway by crossing *Cenpb*<sup>-/-</sup> knockout females<sup>38</sup> to WT

males to generate zygotes lacking a maternal pool of CENP-B protein. Our equalization model predicts that a potential epigenetic contribution to CENP-C recruitment is masked by the genetic pathway, which is symmetric when maternal and paternal centromeres are genetically identical. In the absence of the genetic pathway, CENP-C asymmetry between maternal and paternal centromeres would increase due to the initial epigenetic asymmetry (Fig. 6e,f).



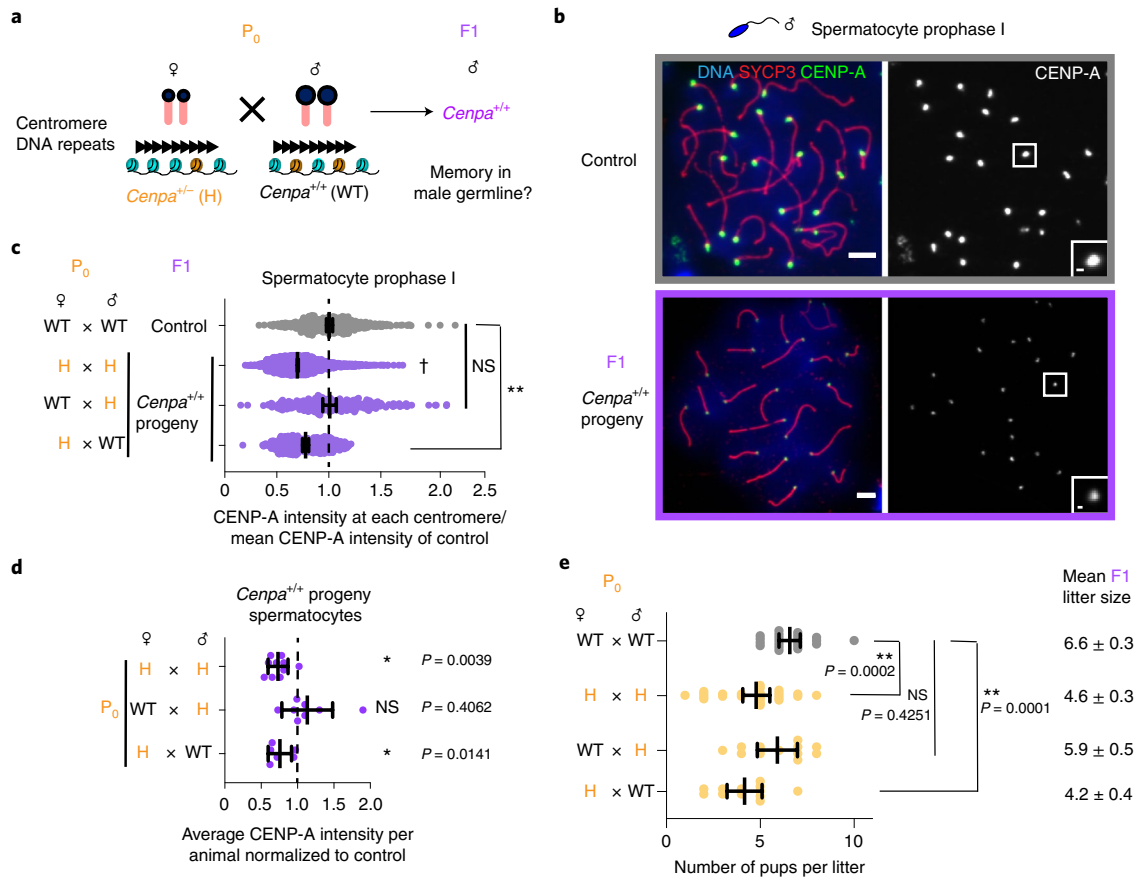


**Fig. 4 | Centromere strength depends on maternally inherited CENP-A.** **a**, Mating scheme to test the *Cenpa* maternal contribution. **b**, Prophase I spermatocytes from control and F1 progeny of the H♀ × WT♂ cross. Each of the CENP-A foci represents four centromeres from a pair of homologous chromosomes. Scale bars, 5  $\mu$ m (main panel) and 1  $\mu$ m (inset). **c**, Quantifications of CENP-A foci intensities in F1 spermatocytes from the indicated crosses. Representative images are shown in Fig. 1d († indicates H × H, data replotted for comparison from Fig. 1c), Fig. 3f (WT♀ × H♂) and **b** (H♀ × WT♂).  $N = 536, 1,836^\dagger, 267$  and 604 centromeres (top to bottom). **d**, Data from **c** replotted by averaging over all centromeres from spermatocytes in each animal, normalized to controls (dashed line).  $N = 10, 8$  and 6 animals (top to bottom). \* $P < 0.05$ ; NS,  $P > 0.05$ ; Wilcoxon signed sum rank test (two-tailed). **e**, Litter sizes from the indicated crosses.  $N = 21, 26, 12$  and 12 litters (top to bottom). Mean  $\pm$  s.e.m. values for each cross are shown next to the graph. \*\* $P < 0.0001$ ; NS,  $P > 0.05$ ; Mann–Whitney U test (two-tailed). Error bars: median  $\pm$  95% CI.

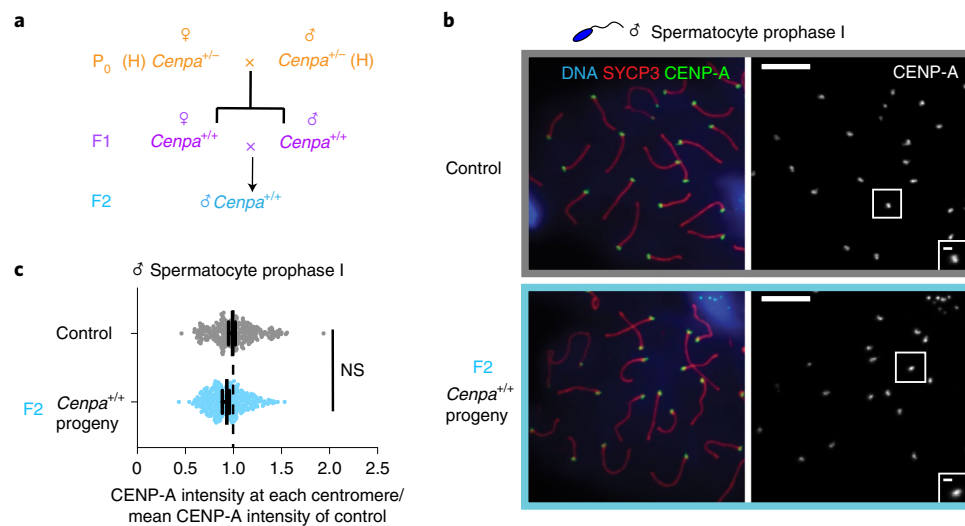


**Fig. 5 | CENP-A chromatin recovers in adult male F2 progeny from *Cenpa*<sup>+/+</sup> WT F1 parents.** **a**, Mating scheme to generate the F2 generation from F1 with epigenetically weakened centromeres and WT genotype. **b**, Prophase I spermatocytes from control and F2 males. Each of the CENP-A foci represents four centromeres from a pair of homologous chromosomes. Scale bars, 5  $\mu$ m (main panel) and 1  $\mu$ m (inset). **c**, Quantification of CENP-A foci intensities.  $N = 276$  (control) and 328 (F2) centromeres. NS,  $P > 0.05$ ; Mann–Whitney U test (two-tailed). Error bars, median  $\pm$  95% CI.

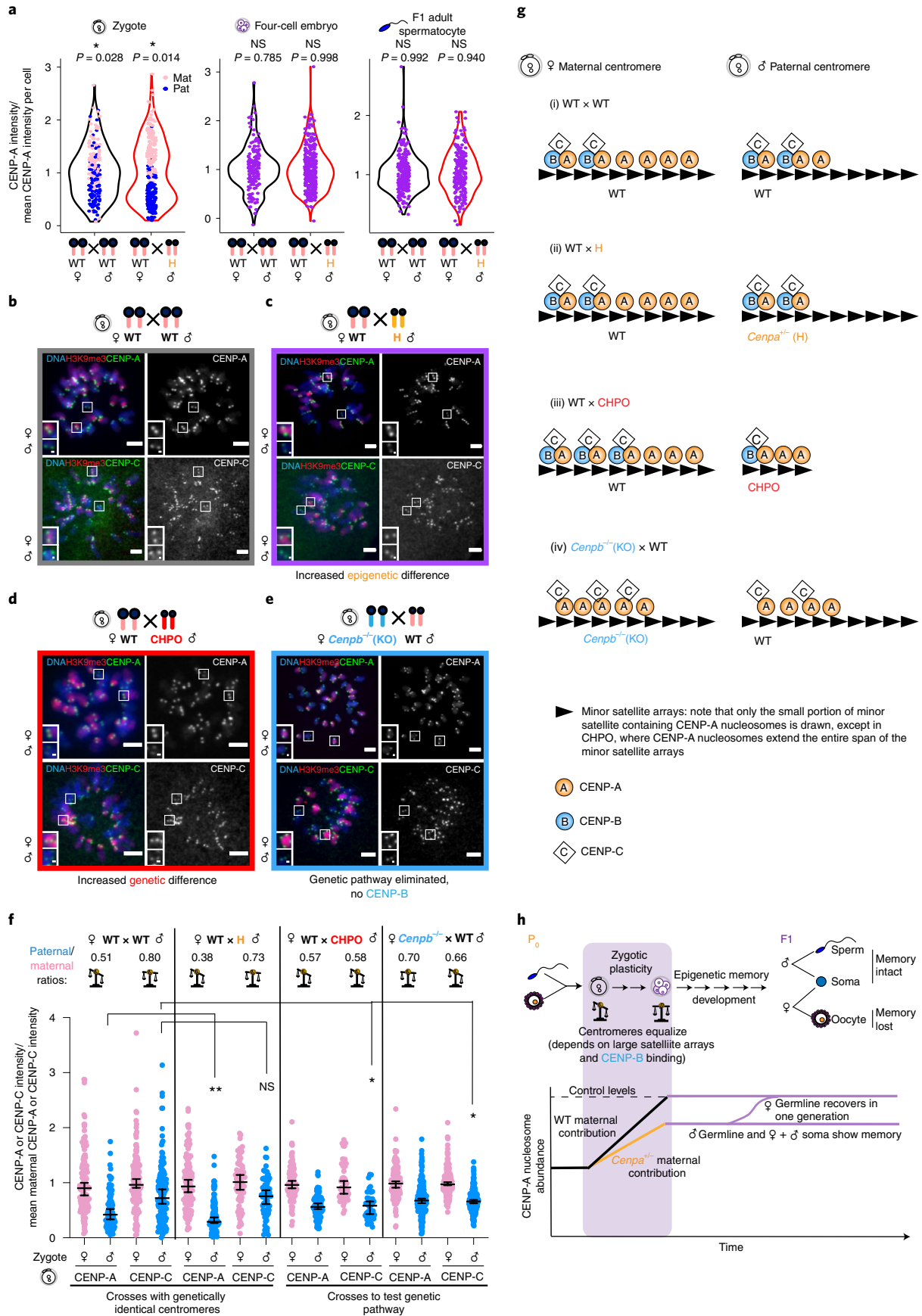


**Fig. 6 | Genetic contributions to centromere equalization in early embryogenesis.** **a**, Combined violin and dot plots for zygotes, four-cell embryos and adult spermatocytes, showing the distributions of CENP-A intensities. Data for zygotes and spermatocytes are replotted from Figs. 3c and 1c, respectively.  $N=192, 271, 164, 322, 240$  and  $214$  centromeres (left to right). Dot plots are coloured for zygotes, where parental origin can be determined. \* = 'modetest'<sup>52</sup> for unimodality (two-tailed). **b,c**, Images of CENP-A or CENP-C staining in zygotes with either moderate (WT  $\times$  WT, **b**) or enhanced (WT  $\varnothing \times$  H $\delta$ , **c**) epigenetic differences between maternal and paternal centromeres, distinguished by H3K9me3. Each pair of CENP-A or CENP-C foci represents sister centromeres in mitosis. **d,e**, Images of CENP-A or CENP-C staining in zygotes from the indicated crosses manipulating the genetic pathway. Scale bars, 5  $\mu$ m (main panel) and 1  $\mu$ m (inset). KO, knockout. **f**, Quantifications of maternal (pink) and paternal (blue) CENP-A and CENP-C intensities in zygotes from the designated crosses, with average paternal/maternal CENP-A or CENP-C ratios above;  $N=132, 90, 162, 157, 123, 112, 76, 66, 120, 116, 54, 45, 164, 172, 218$  and  $217$  centromeres (left to right). \*\* $P < 0.0001$ , \* $P < 0.05$ , Mann-Whitney U test (two-tailed). Error bars, median  $\pm$  95% CI. **g**, Model for epigenetic and genetic contributions to CENP-C binding via CENP-A and CENP-B in zygotes. (i) WT  $\times$  WT cross: maternal centromeres have more CENP-A nucleosomes than paternal centromeres (Fig. 3c), but CENP-B is equally distributed between genetically identical maternal and paternal centromeres. We propose that CENP-B does not occupy all CENP-B boxes, and that CENP-C is limited relative to CENP-A and preferentially binds to CENP-A nucleosomes that are associated with CENP-B, thereby equalizing the maternal and paternal centromeres. Note that only the small portion of minor satellite containing CENP-A-nucleosomes is drawn. (ii) WT  $\times$  H cross: CENP-A nucleosomes are reduced on the paternal chromatin but still enough to recruit CENP-B/C. CENP-A asymmetry increases, but CENP-C remains symmetric. (iii) WT  $\times$  CHPO cross: paternal CHPO centromeres have fewer minor satellite repeats and fewer CENP-B boxes. Most CENP-B therefore associates with maternal centromeres, providing more binding sites for CENP-C and increasing its asymmetry. (iv) *Cenpb*<sup>-/-</sup>  $\times$  WT: CENP-C binds to any available CENP-A nucleosomes, leading to CENP-C asymmetry matching CENP-A asymmetry. **h**, Summary of changes in centromeric chromatin at weakened paternal centromeres with WT zygotic genotype and either WT or reduced maternal contribution. See Discussion. Note that weakened maternal centromeres would presumably lead to similar outcomes but are difficult to experimentally manipulate without also reducing the maternal contribution.

This epigenetic asymmetry is present in the *Cenpb*<sup>-/-</sup>  $\varnothing \times$  WT  $\delta$  cross, although reduced relative to the WT  $\times$  WT control cross (CENP-A ratio =  $0.7 \pm 0.02$ ) because CENP-A chromatin is reduced in oocytes from *Cenpb*<sup>-/-</sup> females<sup>38</sup>. Despite this decrease in epigenetic asymmetry, the asymmetry in CENP-C recruitment increased in the *Cenpb*<sup>-/-</sup>  $\varnothing \times$  WT  $\delta$  cross relative to the control (CENP-C ratio =  $0.66 \pm 0.01$ ; Fig. 6e,f and Extended Data Fig. 9). This result demonstrates that equalization depends on CENP-B. Summarizing the results of our two experiments manipulating the genetic pathway, we created a genetic asymmetry in the WT  $\varnothing \times$  CHPO  $\delta$  cross, which increased CENP-C asymmetry relative to the WT  $\times$  WT control due to the genetic pathway. In contrast, we eliminated the genetic pathway in the *Cenpb*<sup>-/-</sup>  $\varnothing \times$  WT  $\delta$  cross, which increased CENP-C asymmetry relative to the control by unmasking the epigenetic pathway.

At the molecular level, a parsimonious explanation for epigenetic and genetic contributions to the results of the four crosses we performed (Fig. 6b–e) would involve two distinct pools of CENP-A nucleosomes: one associated with CENP-B and the other without CENP-B. If CENP-A nucleosomes are present in excess of CENP-C, and CENP-C preferentially binds the subset of CENP-A nucleosomes that are also bound to CENP-B<sup>37</sup>, then CENP-C recruitment would be dictated by CENP-B (that is, the genetic pathway) (Fig. 6g(i)). Partial reduction of CENP-A nucleosomes on the paternal centromeres, as in our WT  $\varnothing \times$  H $\delta$  cross, would not affect CENP-C recruitment as long as the remaining CENP-A nucleosomes bind CENP-B and are sufficient to bind the available CENP-C (Fig. 6g(ii)). Limiting CENP-B binding to paternal centromeres, as in our WT  $\varnothing \times$  CHPO  $\delta$  cross, increases CENP-C asymmetry because there are fewer paternal CENP-A nucleosomes associated with CENP-B (Fig. 6g(iii)). Finally, in the absence of CENP-B, CENP-C recruitment becomes a simple pairwise interaction with CENP-A, so CENP-C scales relative to the number of CENP-A nucleosomes (Fig. 6g(iv)).

## Discussion

Together, our findings support a model in which centromere strength is initially determined during a phase of early embryonic plasticity. After the plastic phase, weakened centromeres persist in somatic tissue and the male germline (Fig. 6h), even in genetically WT animals (for example, the *Cenpa*<sup>+/+</sup> progeny of *Cenpa*<sup>+/-</sup> mothers). We thus provide evidence for epigenetic memory through development as predicted by the established mechanism for centromere propagation in somatic cells. By contrast, our in vivo model uncovers a different paradigm of transmission between

generations, with *Cenpa* acting as a maternal effect gene to determine centromere strength.

We show that nascent centromere chromatin assembly in the first embryonic cell cycles depends on maternally provided CENP-A rather than the number of pre-existing CENP-A nucleosomes in the gametes, resetting CENP-A chromatin at the same time that reprogramming occurs for other epigenetic information in the embryo<sup>39–44</sup>. This maternal effect process suggests a different form of epigenetic memory for transmission of a weakened centromere state to offspring through the female germline. In nature, we envision that, like all genes, *Cenpa* expression could vary substantially between individuals through epigenetic effects such as differences in promoter methylation. Mothers with attenuated *Cenpa* expression would therefore transmit weakened centromeres to offspring because of the reduced maternal contribution, even with unattenuated *Cenpa* expression in the offspring. This maternal effect process limits memory to a single generation, however, and also eliminates epigenetic differences between maternal and paternal centromeres in the embryo. By contrast, epigenetic memory in flies is a paternal effect<sup>19</sup>, and a genetic contribution to centromere inheritance through sequence-specific DNA-binding proteins is unlikely given that there does not appear to be a counterpart to CENP-B in flies.

We also find that weakened centromeres recover in the female germline, possibly as a mechanism to protect against loss of centromere identity during the prolonged mammalian oocyte prophase arrest, as CENP-A nucleosomes assembled before this arrest last through the reproductive lifespan of the animal<sup>27</sup>. Recovery may also provide a buffer from potential failure in telomere bouquet protection of centromeres in female meiosis<sup>45</sup>. By contrast, CENP-A is removed early in female meiosis in holocentric worms<sup>46</sup>, so de novo assembly is required to re-establish centromere chromatin. Similarly, in worms, *Cenpa* mutants that disrupt interactions with the assembly machinery are maternal effect lethal as they abrogate this de novo assembly<sup>47</sup>.

Epigenetic specification of centromeres may have evolved as a strategy to suppress fitness costs associated with selfish centromere DNA sequences that subvert female meiosis<sup>48</sup> (drive) to increase their transmission to the egg. Epigenetic centromeres require a propagation mechanism, which can impose its own costs, however. If pre-existing CENP-A nucleosomes recruit the machinery for nascent assembly, then epigenetic differences between maternal and paternal centromeres in the zygote can lead to differential assembly. Indeed, epigenetic differences in plants cause embryonic aneuploidy due to loss of weaker centromeres or even complete

elimination of one parental genome<sup>17,49</sup>. Our finding of a specialized early embryonic assembly process, directed by centromere DNA sequence rather than pre-existing CENP-A nucleosomes, reveals a mechanism to equalize centromeres to protect against the detrimental consequence of epigenetic asymmetry between the parental genomes. We propose that dual genetic and epigenetic contributions to centromere chromatin assembly represent adaptations to fitness costs arising from either selfish DNA sequences or parental epigenetic asymmetry.

### Online content

Any methods, additional references, Nature Research reporting summaries, source data, extended data, supplementary information, acknowledgements, peer review information; details of author contributions and competing interests; and statements of data and code availability are available at <https://doi.org/10.1038/s41556-022-00897-w>.

Received: 7 June 2021; Accepted: 16 March 2022;

Published online: 09 May 2022

### References

- Kixmoeller, K., Allu, P. K. & Black, B. E. The centromere comes into focus: from CENP-A nucleosomes to kinetochore connections with the spindle. *Open Biol.* **10**, 200051 (2020).
- Dumont, M. & Fachinetti, D. DNA sequences in centromere formation and function. *Prog. Mol. Subcell. Biol.* **56**, 305–336 (2017).
- Chmátal, L., Schultz, R. M., Black, B. E. & Lampson, M. A. Cell biology of cheating-transmission of centromeres and other selfish elements through asymmetric meiosis. *Prog. Mol. Subcell. Biol.* **56**, 377–396 (2017).
- Iwata-Otsubo, A. et al. Expanded satellite repeats amplify a discrete CENP-A nucleosome assembly site on chromosomes that drive in female meiosis. *Curr. Biol.* **27**, 2365–2373.e8 (2017).
- Akera, T., Trimm, E. & Lampson, M. A. Molecular strategies of meiotic cheating by selfish centromeres. *Cell* **178**, 1132–1144 (2019).
- Fishman, L. & Saunders, A. Centromere-associated female meiotic drive entails male fitness costs in monkeyflowers. *Science* **322**, 1559–1562 (2008).
- Voullaire, L. E., Slater, H. R., Petrovic, V. & Choo, K. H. A. A functional marker centromere with no detectable  $\alpha$ -satellite, satellite III or CENP-B protein: activation of a latent centromere? *Am. J. Hum. Genet.* **52**, 1153–1163 (1993).
- Logsdon, G. A. et al. Human artificial chromosomes that bypass centromeric DNA. *Cell* **178**, 624–639 (2019).
- Depinet, T. W. et al. Characterization of neo-centromeres in marker chromosomes lacking detectable  $\alpha$ -satellite DNA. *Hum. Mol. Genet.* **6**, 1195–1204 (1997).
- Du Sart, D. et al. A functional neo-centromere formed through activation of a latent human centromere and consisting of non- $\alpha$ -satellite DNA. *Nat. Genet.* **16**, 144–153 (1997).
- Black, B. E. & Cleveland, D. W. Epigenetic centromere propagation and the nature of CENP-A nucleosomes. *Cell* **144**, 471–479 (2011).
- Foltz, D. R. et al. Centromere-specific assembly of CENP-A nucleosomes is mediated by HJURP. *Cell* **137**, 472–484 (2009).
- Jansen, L. E. T., Black, B. E., Foltz, D. R. & Cleveland, D. W. Propagation of centromeric chromatin requires exit from mitosis. *J. Cell Biol.* **176**, 795–805 (2007).
- Dunleavy, E. M. et al. HJURP is a cell-cycle-dependent maintenance and deposition factor of CENP-A at centromeres. *Cell* **137**, 485–497 (2009).
- Schuh, M., Lehner, C. F. & Heidmann, S. Incorporation of *Drosophila* CID/CENP-A and CENP-C into centromeres during early embryonic anaphase. *Curr. Biol.* **17**, 237–243 (2007).
- Moree, B., Meyer, C. B., Fuller, C. J. & Straight, A. F. CENP-C recruits M18BP1 to centromeres to promote CENP-A chromatin assembly. *J. Cell Biol.* **194**, 855–871 (2011).
- Ravi, M. & Chan, S. W. L. Haploid plants produced by centromere-mediated genome elimination. *Nature* **464**, 615–618 (2010).
- Comai, L. & Tan, E. H. Haploid induction and genome instability. *Trends Genet.* **35**, 791–803 (2019).
- Raychaudhuri, N. et al. Transgenerational propagation and quantitative maintenance of paternal centromeres depends on Cid/Cenp-A presence in *Drosophila* sperm. *PLoS Biol.* **10**, e1001434 (2012).
- Gassmann, R. et al. An inverse relationship to germline transcription defines centromeric chromatin in *C. elegans*. *Nature* **484**, 534–537 (2012).
- Liu, H., Kim, J. M. & Aoki, F. Regulation of histone H3 lysine 9 methylation in oocytes and early pre-implantation embryos. *Development* **131**, 2269–2280 (2004).
- Burton, A. et al. Heterochromatin establishment during early mammalian development is regulated by pericentromeric RNA and characterized by non-repressive h3k9me3. *Nat. Cell Biol.* **22**, 767–778 (2020).
- Puschendorf, M. et al. PRC1 and Suv39h specify parental asymmetry at constitutive heterochromatin in early mouse embryos. *Nat. Genet.* **40**, 411–420 (2008).
- Palmer, D. K., O'Day, K. & Margolis, R. L. The centromere specific histone CENP-A is selectively retained in discrete foci in mammalian sperm nuclei. *Chromosoma* **100**, 32–36 (1990).
- Palmer, D. K., Day, K. O., Trongt Le, H., Charbonneau, H. & Margolis, R. L. Purification of the centromere-specific protein CENP-A and demonstration that it is a distinctive histone. *Proc. Natl Acad. Sci. USA* **88**, 3734–3738 (1991).
- Brinkley, B. R. et al. Arrangements of kinetochores in mouse cells during meiosis and spermiogenesis. *Chromosoma* **94**, 309–317 (1986).
- Smoak, E. M., Stein, P., Schultz, R. M., Lampson, M. A. & Black, B. E. Long-term retention of CENP-A nucleosomes in mammalian oocytes underpins transgenerational inheritance of centromere identity. *Curr. Biol.* **26**, 1110–1116 (2016).
- Richter, J. D. Cytoplasmic polyadenylation in development and beyond. *Microbiol. Mol. Biol. Rev.* **63**, 446–456 (1999).
- Zeng, F., Baldwin, D. A. & Schultz, R. M. Transcript profiling during preimplantation mouse development. *Dev. Biol.* **272**, 483–496 (2004).
- Ishiyuchi, T. et al. Reprogramming of the histone H3.3 landscape in the early mouse embryo. *Nat. Struct. Mol. Biol.* **28**, 38–49 (2021).
- Barnhart, M. C. et al. HJURP is a CENP-A chromatin assembly factor sufficient to form a functional de novo kinetochore. *J. Cell Biol.* **194**, 229–243 (2011).
- Fujita, Y. et al. Priming of centromere for CENP-A recruitment by human hmis18 $\alpha$ , hmis18 $\beta$  and M18BP1. *Dev. Cell* **12**, 17–30 (2007).
- Nardi, I. K., Zasadzińska, E., Stellfox, M. E., Knippler, C. M. & Foltz, D. R. Licensing of centromeric chromatin assembly through the Mis18 $\alpha$ -Mis18 $\beta$  heterotetramer. *Mol. Cell* **61**, 774–787 (2016).
- Stellfox, M. E., Nardi, I. K., Knippler, C. M. & Foltz, D. R. Differential binding partners of the Mis18 $\alpha$ / $\beta$  YIPPEE domains regulate Mis18 complex recruitment to centromeres. *Cell Rep.* **15**, 2127–2135 (2016).
- Bodor, D. L. et al. The quantitative architecture of centromeric chromatin. *eLife* **3**, e02137 (2014).
- Masumoto, H., Masukata, H., Muro, Y., Nozaki, N. & Okazaki, T. A human centromere antigen (CENP-B) interacts with a short specific sequence in alphoid DNA, a human centromeric satellite. *J. Cell Biol.* **109**, 1963–1973 (1989).
- Fachinetti, D. et al. DNA sequence-specific binding of CENP-B enhances the fidelity of human centromere function. *Dev. Cell* **33**, 314–327 (2015).
- Kumon, T. et al. Parallel pathways for recruiting effector proteins determine centromere drive and suppression. *Cell* **184**, 4904–4918 (2021).
- Rossant, J. Postimplantation development of blastomeres isolated from 4 and 8 cell mouse eggs. *J. Embryol. Exp. Morphol.* **36**, 283–290 (1976).
- Lepikhov, K. & Walter, J. Differential dynamics of histone H3 methylation at positions K4 and K9 in the mouse zygote. *BMC Dev. Biol.* **4**, 12 (2004).
- Lepikhov, K. et al. Evidence for conserved DNA and histone H3 methylation reprogramming in mouse, bovine and rabbit zygotes. *Epigenetics Chromatin* **1**, 8 (2008).
- Xu, Q. & Xie, W. Epigenome in early mammalian development: inheritance, reprogramming and establishment. *Trends Cell Biol.* **28**, 237–253 (2018).
- Xie, B. et al. Histone H3 lysine 27 trimethylation acts as an epigenetic barrier in porcine nuclear reprogramming. *Reproduction* **151**, 9–16 (2016).
- Van Der Heijden, G. W. et al. Asymmetry in histone H3 variants and lysine methylation between paternal and maternal chromatin of the early mouse zygote. *Mech. Dev.* **122**, 1008–1022 (2005).
- Hou, H. et al. Centromeres are dismantled by foundational meiotic proteins Spo11 and Rec8. *Nature* **591**, 671–676 (2021).
- Monen, J., Maddox, P. S., Hyndman, F., Oegema, K. & Desai, A. Differential role of CENP-A in the segregation of holocentric *C. elegans* chromosomes during meiosis and mitosis. *Nat. Cell Biol.* **7**, 1248–1255 (2005).
- Prosée, R. F. et al. Trans-generational inheritance of centromere identity requires the CENP-A N-terminal tail in the *C. elegans* maternal germ line. *PLoS Biol.* **19**, e3000968 (2021).
- Malik, H. S. & Henikoff, S. Major evolutionary transitions in centromere complexity. *Cell* **138**, 1067–1082 (2009).
- Maheshwari, S. et al. Naturally occurring differences in CENH3 affect chromosome segregation in zygotic mitosis of hybrids. *PLoS Genet.* **11**, e1004970 (2015).
- Bao, J. & Bedford, M. T. Epigenetic regulation of the histone-protamine transition during spermiogenesis. *Reproduction* **151**, R55–R70 (2016).
- Rathke, C., Baarends, W. M., Awe, S. & Renkawitz-Pohl, R. Chromatin dynamics during spermiogenesis. *Biochim. Biophys. Acta* **1839**, 155–168 (2014).
- Ameijeiras-Alonso, J., Crujeiras, R. M. & Rodríguez-Casal, A. Mode testing, critical bandwidth and excess mass. *Test* **28**, 900–919 (2019).

**Publisher's note** Springer Nature remains neutral with regard to jurisdictional claims in published maps and institutional affiliations.

© The Author(s), under exclusive licence to Springer Nature Limited 2022

## Methods

**Animal husbandry and generation of *Cenpa*<sup>+/-</sup> heterozygous and *Cenpb*<sup>-/-</sup> knockout mice.** All animal experiments and protocols were approved by the Institutional Animal Use and Care Committee of the University of Pennsylvania and were consistent with National Institutes of Health guidelines (protocol #803994). All animals used in this study were within six months of age, and both male and female animals were analysed. Experimental animals were compared to age- and gender-matched controls. *Cenpa*<sup>+/-</sup> heterozygous (H) mice were initially generated by mating *Cenpa*<sup>fl/fl</sup>; *Gdf9Cre/+* conditional *Cenpa* knockout females with WT males<sup>27</sup> (C57BL/6J, Jackson Laboratory, 000664) and subsequently regenerated through either WT♀ × H♂, H × H or H♀ × WT♂ crosses, which also generated the experimental *Cenpa*<sup>+/-</sup> F1 progeny. F1 control progeny were generated by mating *Cenpa*<sup>fl/fl</sup> females to WT C57BL/6J males. 'CHPO' males were obtained from Jackson Laboratory (ZALENDE/Eij, 001392) and then bred in house. For each dataset, at least two to five independent experiments were performed, each having one control and one to two experimental animals that were age- and gender-matched. For embryo collections, five to eight females were mated to five to eight males for each independent experiment. Genotyping for *Cenpa* was performed using the REDEExtract N-AMP kit (Sigma)<sup>27</sup> and all animals were sampled twice to confirm their genotype. *Cenpb*<sup>-/-</sup> mice were generated in a CF-1/C57BL/6J/DBA-2 hybrid strain using CRISPR-Cas9 genome editing<sup>38</sup>.

**Microscopy.** Confocal images were collected as z-stacks with 0.5-μm intervals, using a microscope (DMI4000 B; Leica) equipped with a ×63 1.3-NA glycerol-immersion objective lens, an x-y piezo Z stage (Applied Scientific Instrumentation), a spinning disk confocal scanner (Yokogawa Corporation of America), an electron-multiplying charge-coupled device camera (ImageEM C9100-13; Hamamatsu Photonics) and either an LMM5 (Spectral Applied Research) or Versalase (Vortran Laser Technology) laser merge module, controlled by MetaMorph software (Molecular Devices, v7.10.3.294). Images were acquired using the same laser settings and all images in a panel were scaled the same. Single channels are shown wherever quantifications were performed.

**Oocyte collection and culture.** Female mice were hormonally primed with 5 U of pregnant mare serum gonadotropin (PMSG, Peptides International) 44–48 h before oocyte collection. Germinal vesicle intact oocytes were collected in bicarbonate-free minimal essential medium<sup>53</sup> (M2, Sigma), denuded from cumulus cells, and cultured in Chatot-Ziomek-Bavister<sup>53</sup> (CZB, Fisher Scientific) medium covered with mineral oil (Sigma, BioXTRA) in a humidified atmosphere of 5% CO<sub>2</sub> in air at 37°C. During collection, meiotic resumption was inhibited by addition of 2.5 mM milrinone (Sigma). Milrinone was subsequently washed out to allow meiotic resumption and oocytes were fixed 6–7 h later at metaphase I.

**Oocyte immunocytochemistry.** Oocytes were fixed in freshly prepared 2% paraformaldehyde (Sigma) in phosphate buffered saline (PBS) with 0.1% Triton X-100 (Sigma), pH 7.4, for 20 min at room temperature (r.t.), permeabilized in PBS with 0.2% Triton X-100 for 15 min at r.t., placed in blocking solution (PBS containing 0.3% bovine serum albumin (BSA) and 0.01% Tween-20) overnight at 4°C, treated with λ-phosphatase (1,600 U, NEB) for 1 h at 30°C for CENP-A staining, incubated for 1 h with primary antibody in blocking solution, washed three times for 10 min each, incubated for 1 h with secondary antibody, washed three times for 10 min each, and mounted in Vectashield with 4',6-diamidino-2-phenylindole (DAPI; Vector) to visualize the chromosomes. The primary antibody was rabbit anti-mouse CENP-A (1:200, Cell Signaling, C51A7). The secondary antibody was donkey anti-rabbit Alexa Fluor 488 (1:500, Invitrogen).

**Sucrose spreading of mouse spermatocyte chromosomes.** A modification of a previous chromosome spreading protocol was used<sup>39</sup>. Mouse testes were collected from males, and individual seminiferous tubules were transferred to 3 ml of ice-cold freshly made hypotonic buffer for 60 min. Small sections of tubules were placed on depression slides in 22 μl of 100 mM sucrose (pH 8.2) and minced with two scalpel blades until most of the tubules were cut and the liquid was cloudy. Any large chunks of tubules were removed and another 22 μl of sucrose was added and mixed with the sample, followed by spreading 30 μl of cell suspension on slides dipped into freshly made 1% paraformaldehyde (PFA; 0.15% Triton X-100 in dH<sub>2</sub>O). Slides were then placed directly into a humidified chamber covered with a lid. After 2.5 h, the lid was left half-open for an additional 30 min. After drying, slides were washed twice in Photoflo/PBS for 5 min followed by antibody staining, or frozen at -80°C.

**Spermatocyte immunocytochemistry.** Mouse spermatocytes were spread on glass slides as described in the above section, then incubated for 10 min at r.t. in 0.4% Photoflo (Fisher Scientific)/PBS, followed by 10 min in 0.01% Triton-X-100/PBS and 10 min in antibody dilution buffer (ADB)/PBS (3 g BSA, 10 ml of goat serum, 250 μl of 20% Triton X-100 in 1 l of PBS). For metaphase cells, slides were treated with λ-phosphatase (1,600 U, NEB) for 1 h at 30°C. Slides were incubated on parafilm runners, with rabbit anti-CENP-A antibody (1:400) and mouse anti-SYCP3 antibody (1:200, Abcam, 10G11/7), overnight at r.t. in a humidified chamber, washed for 10 min in Photoflo/PBS, Triton X/PBS and ADB/PBS sequentially, and incubated for 1.5 h at 37°C with donkey anti-mouse Alexa

Fluor 594 (1:100, Invitrogen) and donkey anti-rabbit Alexa Fluor 488 (1:2,000, Invitrogen) secondary antibodies. The slides were then washed three times for 10 min each, with 0.4% Photoflo/PBS and once with 0.4% Photoflo/dH<sub>2</sub>O for 10 min, and mounted with Vectashield with DAPI (Vector) on a 24 × 40-mm cover glass. From each slide, primary spermatocytes at either pachytene stage (overall CENP-A levels) or diplotene stage (bivalent analysis of ratios) of prophase I were selected based on the distinct SYCP3 staining pattern (paired and threadlike in pachytene and X-shaped in diplotene after synaptonemal complex disassembly) and imaged using the confocal microscope described in the Microscopy section.

**Bone marrow collection and immunocytochemistry.** Bone marrow was collected from the tibia(s) and femur(s) by inserting a 26-G syringe needle into the cut end of the marrow cavity. Cells were flushed out into 1 ml of warm ethylenediaminetetraacetic acid (EDTA) buffer (8 g sodium chloride, 0.2 g potassium dihydrophosphate, 0.2 g potassium chloride, 1.15 g sodium dihydrophosphate, 0.2 g EDTA, dissolved in 1 l of deionized water) with 0.025% colchicine (Sigma) and incubated for 3 h at 37°C. Cells were then diluted 50 times in 0.56% potassium chloride solution on ice for 20 min to swell. Spreads were subsequently prepared on Superfrost Plus slides using a double funnel on a Cytospin 4 cytocentrifuge (ThermoFisher) at 600 r.p.m., high acceleration for 5 min, then rinsed briefly in PBS and fixed in 4% formaldehyde solution for 20 min at r.t., permeabilized in 0.5% Triton X-100/PBS and blocked for 20 min (0.3% BSA, 0.01% Tween-20). The slides were incubated with anti-CENP-A antibody (1:200) for 1 h at r.t., washed three times with PBST (PBS/0.01% Tween-20), incubated with donkey anti-rabbit Alexa Fluor 488 (1:500, Invitrogen) for 1 h at r.t., washed three times in PBST for 5 min each and once in distilled water, and then mounted in Vectashield with DAPI to visualize chromosomes.

**Collection of embryos and in vitro fertilization.** C57BL/6J or *Cenpb*<sup>-/-</sup> females were hormonally primed with 5 U of PMSG (Peptides International) and the oocytes were matured in vivo with 5 U of human chorionic gonadotropin (hCG; Sigma) before mating with either C57BL/6J (WT) or *Cenpa*<sup>+/-</sup> males. Because the *Cenpa*<sup>+/-</sup> males have low mating efficiency they were fed a special low soymeal diet (5LG4 irradiated diet, Labdiet) before mating. Embryos were collected 14–16 h post hCG in M2 containing hyaluronidase (0.3 mg ml<sup>-1</sup>) to remove cumulus cells and subsequently washed in M2 (Sigma) and cultured in EmbryoMax Advanced KSOM (AKSOM, Millipore Sigma) with humidified air and 5% CO<sub>2</sub>. Next, 5 μM proTAME (R&D systems) was added at 4 h or ~32–34 h post collection to arrest embryos at one-cell or four-cell mitosis, respectively. Chromosomes were dispersed by generating a monopolar spindle using 10 μM S-trityl-L-cysteine (STLC; Sigma) for 3 h. For experiments using males with limited efficiency of overnight mating (CHPO or *Cenpa*<sup>+/-</sup>), we obtained embryos by in vitro fertilization (IVF), modified from a previously established protocol<sup>36</sup>. Notably, paternal/maternal CENP-A ratios for controls from IVF and in vivo fertilized embryos were comparable. Briefly, sperm from the cauda epididymis were collected from two- to four-month-old males in 500 μl of EmbryoMax human tubal fluid (HTF; Millipore Sigma) and allowed to swim out for 15 min. Sperm were capacitated for 2 h in 2-ml swim up tubes in HTF, before fertilization. Females were primed with PMSG and hCG as described above. MII eggs were collected 14–15 h post hCG into M2 and then transferred into a 50-μl fertilization drop of HTF. Sperm were added to a final concentration of 100,000 sperm per drop for 3 h. Fertilized eggs were washed through AKSOM and cultured overnight at 37°C in humidified air with 5% CO<sub>2</sub>. Embryos were arrested in mitosis as described above.

**Embryo immunocytochemistry.** Embryos were fixed in 2% formaldehyde solution in PBS with 0.1% Triton X-100 for 20 min at r.t., permeabilized in PBS with 0.5% Triton X-100 for 15 min at r.t., placed in blocking solution (PBS containing 0.3% BSA and 0.01% Tween-20) overnight at 4°C or at r.t. for 20 min, treated with λ-phosphatase for 1 h at 30°C for CENP-A and H3K9me3 staining, incubated for 1 h with primary antibodies in blocking solution, washed three times for 15 min, incubated for 1 h with secondary antibodies, washed three times for 15 min, and mounted in Vectashield with DAPI (Vector) to visualize chromosomes. The primary antibodies used were anti-CENP-A (1:200), mouse anti-human H3K9me3 (1:500, Active motif, 2AG-6F12-H4) and a custom polyclonal antibody raised against mouse CENP-C. Briefly, a New Zealand White rabbit was immunized using purified GST-tagged mouse CENP-C (aa 1–198) in PBS as an antigen and Freund's adjuvant. The serum was then used at a concentration of 1:1,000 in embryos. The secondary antibodies used were donkey anti-rabbit Alexa Fluor 488 (1:500, Invitrogen) and donkey anti-mouse Alexa Fluor 594 (1:500, Invitrogen).

**Quantification of centromere signals.** To quantify centromere signal ratios, a sum intensity Z-projection was made using Fiji/ImageJ software. Circles of constant diameter were drawn around individual centromeres and the average intensity was calculated for each centromere after subtracting background, obtained from nearby regions. Raw centromere intensities were obtained from several controlled independent experiments (two or three) and multiple cells were analysed from each animal. Normalization of centromere intensities was performed using age- and gender-matched controls for each independent experiment. For elongating spermatids, we quantified total CENP-A levels per cell instead of individual foci, because the centromeres are clustered.

**Statistics and reproducibility.** All statistical tests for significance were performed in GraphPad Prism 9 or R<sup>56</sup>. *P* values were calculated at a significance ( $\alpha$ ) level of 0.05 (95% confidence interval (CI)) and all tests performed were two-tailed. No statistical method was used to predetermine sample size. Randomization is built into our experiments as each animal was chosen from a different litter and mating pair, no data were excluded and all cells were imaged at random. Samples were designated as control or experiment according to their genotyping data. Animals were genotyped twice. Within a genotype, animals were randomly picked. Because our experiment was with a heterozygous single deletion within the genome, we did not have any covariates to consider. Investigators were not blinded for data collection (imaging) and quantifications (data analysis) as the phenotype automatically reports on the genotype consistently and is very penetrant. Similarly, statistical analysis of bimodality did not require blinding because the rotated kernel density (violin) plots being analysed showed obvious bi/unimodality in each cross. Graphs were created with GraphPad Prism 9 or R. For all quantified experiments, the numbers of replicates (animals or independent experiments) are provided in Supplementary Table 1. Bimodality testing was performed using the R package<sup>57,58</sup> 'multimode' with the function 'modetest' (Fig. 6a) using the excess mass statistic with bootstrapping at a significance ( $\alpha$ ) level of 0.05 (95% CI). A subset from the F1 adult spermatocyte data was used as a representative control unimodal distribution for comparison (Fig. 6a).  $P < 0.05$  from the test indicates that the distributions are significantly non-unimodal. Using results from 'modetest', the location of the modes and the density of each mode per distribution were determined and plotted with the 'locomodes' function (Extended Data Fig. 8).

**Analysis of the 3' UTR of *Cenpa*.** The consensus sequences for CPEI and CPEII were found by manual evaluation of 3' UTR sequences of *Cenpa* from the NCBI database for annotated transcripts. The multiple sequence alignment (MAFFT V7) of the 12 rodent 3' UTRs were made and annotated with UGene (Unipro V37).

**Reporting Summary.** Further information on research design is available in the Nature Research Reporting Summary linked to this Article.

### Data availability

Previously published microarray data for long poly-(A) tailed *Cenpa* mRNA in pre-implantation development is available freely on the NCBI Gene Expression Omnibus (GEO) database (accession no. GDS813 from reference series GSE1749). The 12 mouse genomes used for *Cenpa* 3' UTR analysis are available from the NCBI BioProject database (<https://www.ncbi.nlm.nih.gov/bioproject>) under accession no. PRJNA669840. Data supporting the findings of this study are available from the corresponding author on reasonable request. Source data are provided with this paper.

### Code availability

All codes used for statistical and distribution analysis are freely available as part of the R package 'multimode', described in ref.<sup>58</sup>.

### References

- Stein, P. & Schindler, K. Mouse oocyte microinjection, maturation and ploidy assessment. *J. Vis. Exp.* **53**, 2851 (2011).
- Chatot, C. L., Ziomek, C. A., Bavister, B. D., Lewis, J. L. & Torres, I. An improved culture medium supports development of random-bred 1-cell mouse embryos in vitro. *J. Reprod. Fertil.* **86**, 679–688 (1989).
- Dia, F., Strange, T., Liang, J., Hamilton, J. & Berkowitz, K. M. Preparation of meiotic chromosome spreads from mouse spermatocytes. *J. Vis. Exp.* **129**, 55378 (2017).
- Taft, R. In vitro fertilization in mice. *Cold Spring Harb. Protoc.* <https://doi.org/10.1101/pdb.prot094508> (2017).
- R: a Language and Environment for Statistical Computing (R Foundation for Statistical Computing, 2017).
- Ameijeiras-Alonso, J., Crujeiras, R. M. & Rodriguez-Casal, A. multimode: An R Package for Mode Assessment. *J. Stat. Soft.* **97**, 1–32 (2021).

### Acknowledgements

We thank D. P. Dudka, V. Fu and M. Barmada for assistance with genotyping, G. Logsdon for cloning a protein expression vector, M. Gerace for antigen preparation, D. P. Dudka for help with multiple sequence alignments and R. M. Schultz, M. S. Bartolomei and M. T. Levine for comments and discussion. This work was supported by the NIH (HD058730 to B.E.B. and M.A.L.).

### Author contributions

A. Das contributed to experiments, quantifications, data analysis and statistical analysis, animal husbandry and genotyping. A.I.-O. carried out experiments and quantification for some of Fig. 3g. J.D.-M. prepared and characterized new reagents and assisted with statistical analysis. A. Destouni performed the initial experimentation in zygotes and early embryos. K.G.B. carried out animal husbandry and genotyping. A. Das, B.E.B. and M.A.L. contributed to experimental design, data interpretation and writing. B.E.B. and M.A.L. provided supervision and sourced funding.

### Competing interests

The authors declare no competing interests.

### Additional information

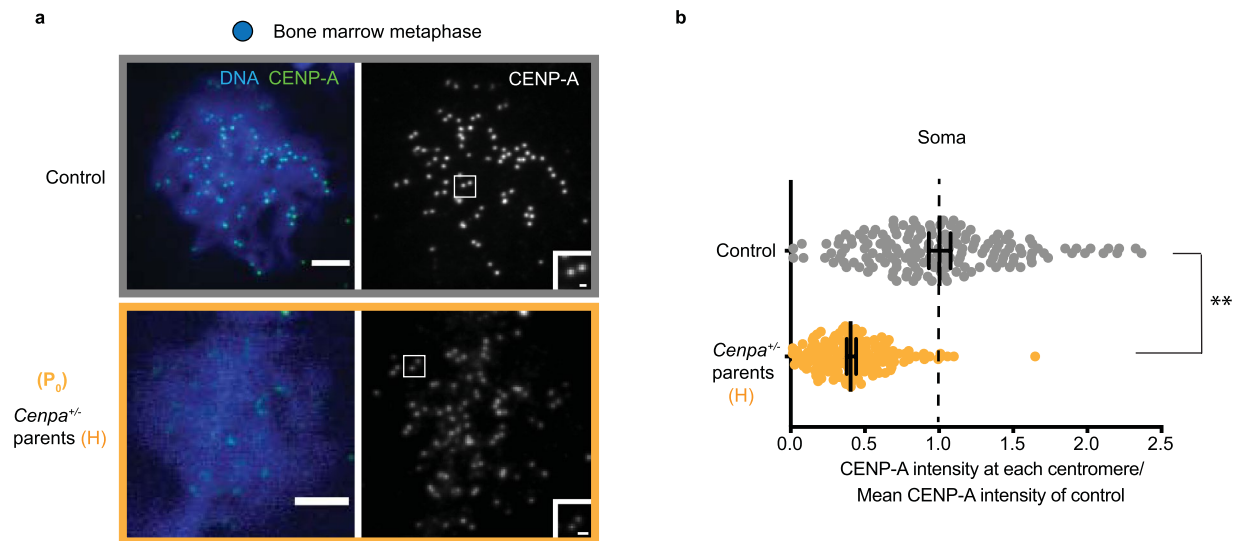
**Extended data** is available for this paper at <https://doi.org/10.1038/s41556-022-00897-w>.

**Supplementary information** The online version contains supplementary material available at <https://doi.org/10.1038/s41556-022-00897-w>.

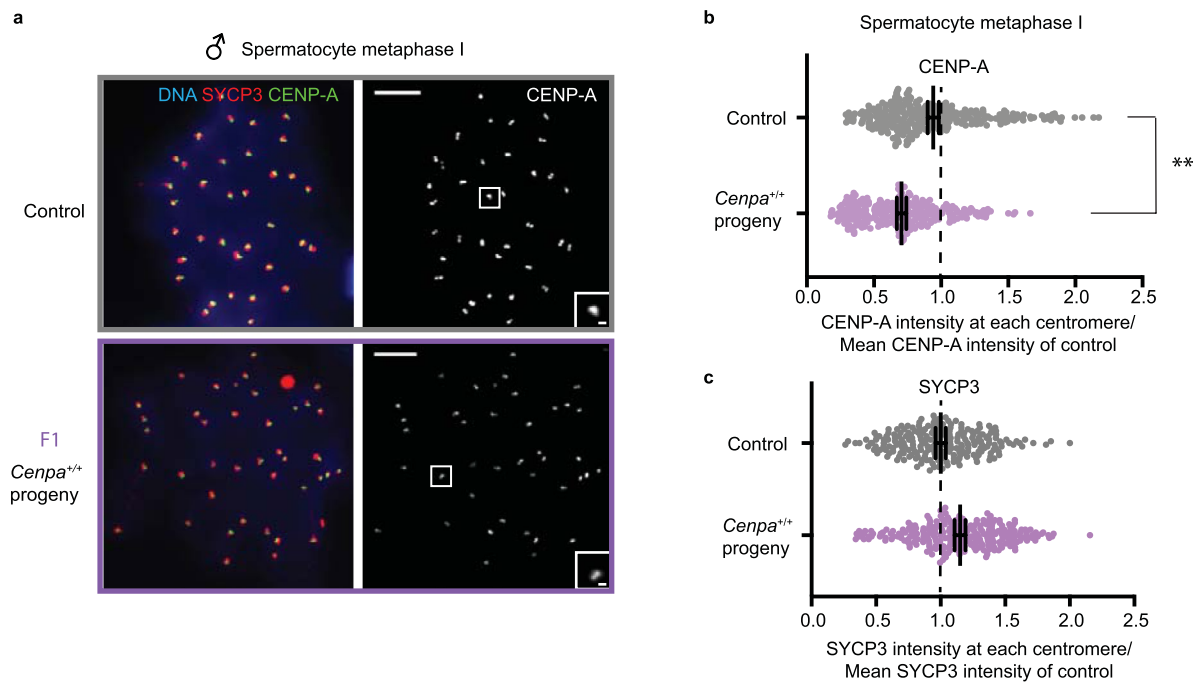
**Correspondence and requests for materials** should be addressed to Ben E. Black or Michael A. Lampson.

**Peer review information** *Nature Cell Biology* thanks Hiroshi Kimura and the other, anonymous, reviewer(s) for their contribution to the peer review of this work.

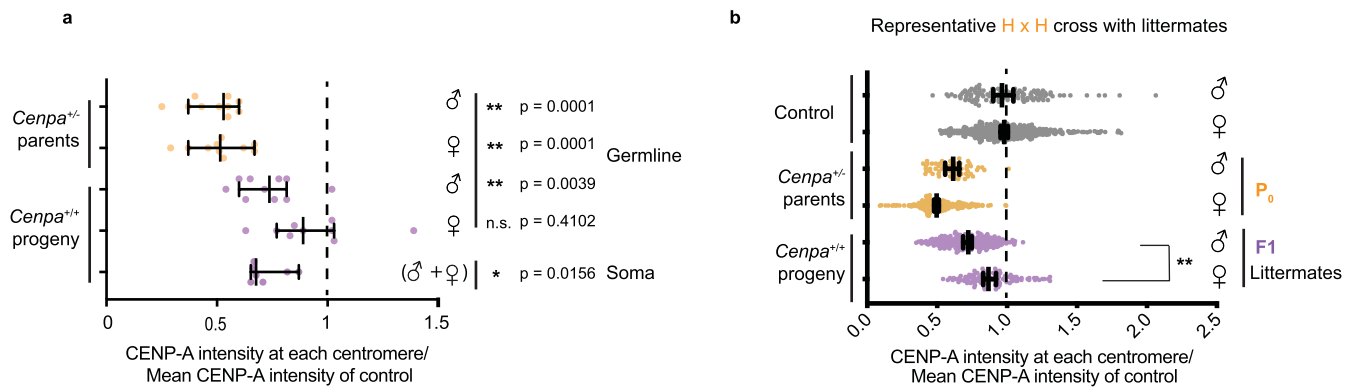
**Reprints and permissions information** is available at [www.nature.com/reprints](http://www.nature.com/reprints).



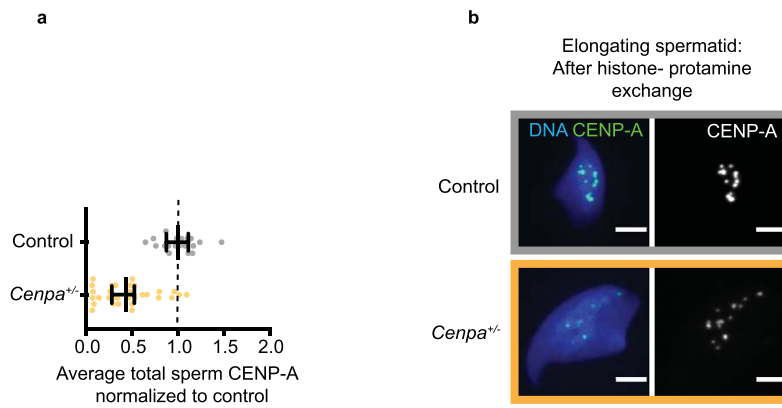
**Extended Data Fig. 1 | CENP-A chromatin is reduced in the soma of *Cenpa*<sup>+/-</sup> heterozygous animals in the P<sub>0</sub> generation. **a**, Bone marrow metaphase spreads: each pair of CENP-A foci represents sister centromeres in mitosis. Scale bars: 5  $\mu$ m (main panel), 1  $\mu$ m (inset). **b**, Quantification of CENP-A foci intensities in control (grey) and P<sub>0</sub> (yellow) generation in soma. N = 166, 170 centromeres (top to bottom). \*\* P < 0.0001, Mann-Whitney U test (two-tailed). Error bars: median  $\pm$  95% CI. Source numerical data are available in source data.**



**Extended Data Fig. 2 | Weakened centromeres in the male germline are independent of meiotic stage.** . Because oocytes were analysed at metaphase I and spermatocytes at prophase I (Fig. 1), we confirmed that F1 spermatocytes also show weakened centromeres at metaphase I. Images (**a**) and quantification (**b**) of F1 spermatocytes show CENP-A reduced to a similar level at metaphase I ( $70.54 \pm 7.1\%$  of control) as prophase I. Each of the CENP-A foci represents four centromeres (a pair of homologous chromosomes, each with two sisters).  $N = 330$  (control), 284 (F1 progeny). Scale bars:  $5 \mu\text{m}$  (main panel),  $1 \mu\text{m}$  (inset). Quantification of SYCP3 foci from the same cells (**c**) shows no decrease ( $114.90 \pm 5.6\%$  of control).  $N = 235$  (control), 259 (F1 progeny). \*\*  $P < 0.001$ , Mann-Whitney U Test (two-tailed). Error bars: median  $\pm$  95% CI. Source numerical data are available in source data.



**Extended Data Fig. 3 | Littermate analysis showing that weakened centromeres persist in the male but not female germline. a**, Data from Fig. 1c replotted as CENP-A levels per animal, averaged over all centromeres in each animal and normalized to controls (dashed line). N = 10, 10, 10, 9, 7 animals. The F1 male but not the female germline and the male and female soma are significantly lower than the controls \*\*P < 0.001, \*P < 0.05 n.s.: P > 0.05, Wilcoxon signed sum rank test (two-tailed). **b**, CENP-A quantifications in spermatocytes and oocytes from littermates from one set of parents. N = 121, 431, 60, 259, 246, 105 centromeres (top to bottom). Female germline levels are significantly elevated compared to littermate male germline levels. \*\*P < 0.0001, Mann-Whitney U Test (two-tailed). Error bars: median ± 95% CI. Source numerical data are available in source data.



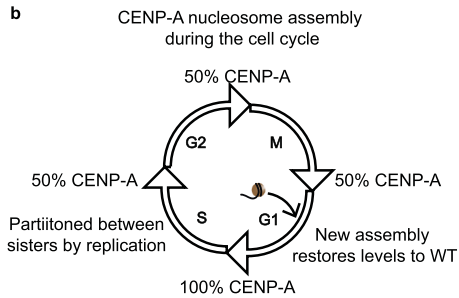
**Extended Data Fig. 4 | CENP-A nucleosomes are retained through the replacement of canonical nucleosomes with protamines during spermiogenesis.**

**a**, Quantification and **b**, images showing CENP-A levels are reduced to  $42.7 \pm 1.5\%$  in spermatids from *Cenpa*<sup>+/-</sup> males compared to WT males, similar to the reduction measured in prophase spermatocytes (Fig. 1c). N = 20 (control), 32 (*Cenpa*<sup>+/-</sup>) spermatids. Error bars: median  $\pm$  95% CI. Scale bars: 5  $\mu$ m (main panel), 1  $\mu$ m (inset). Source numerical data are available in source data.

## a Assumptions:

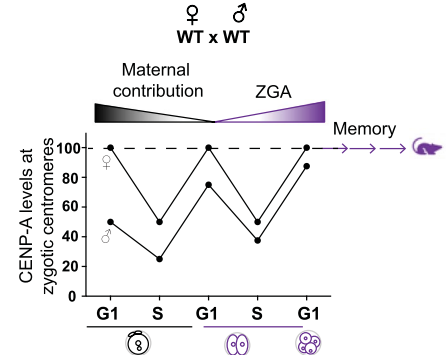
1. New assembly is reduced by 50% in zygotes with heterozygous mothers due to reduced maternal contribution in the first cell cycle.
2. Maternal and paternal centromeres assemble equal amounts.
3. Weakened centromeres persist by epigenetic memory after the first two cell cycles even after activation of a wild type zygotic genome (ZGA)

## b

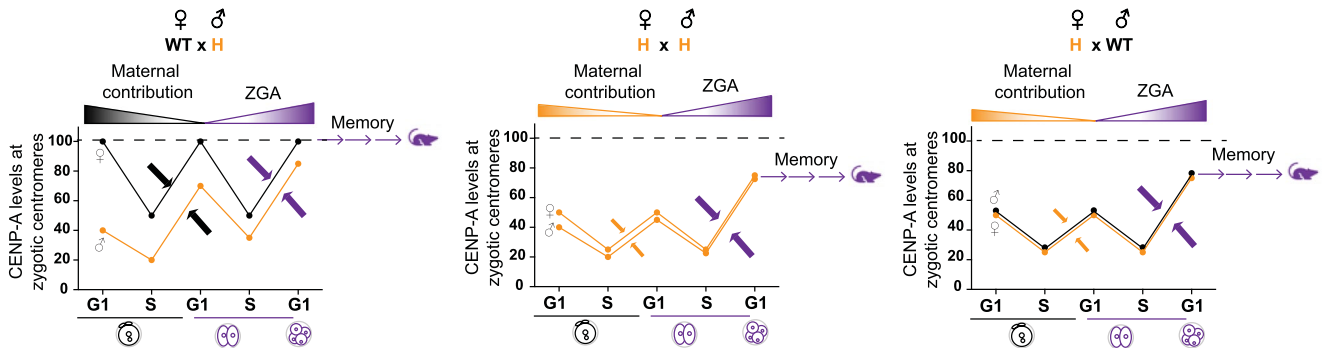


## c Example calculation for projected values in graph for WT x WT:

CENP-A levels		
♀	♂	
G1	100	50 Initial
S	50	25 Diluted by replication
G1	100	75 Reload equal amounts
S	50	37.5 Diluted by replication
G1	100	87.5 Reload equal amounts



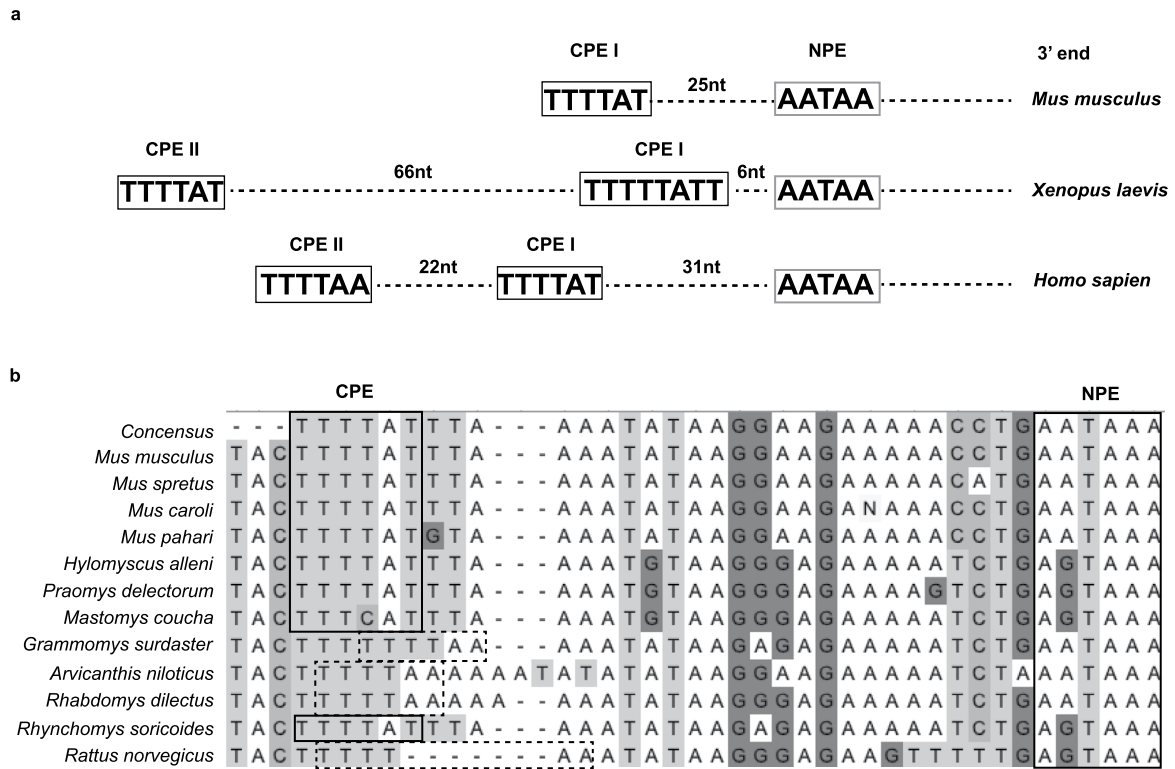
## d



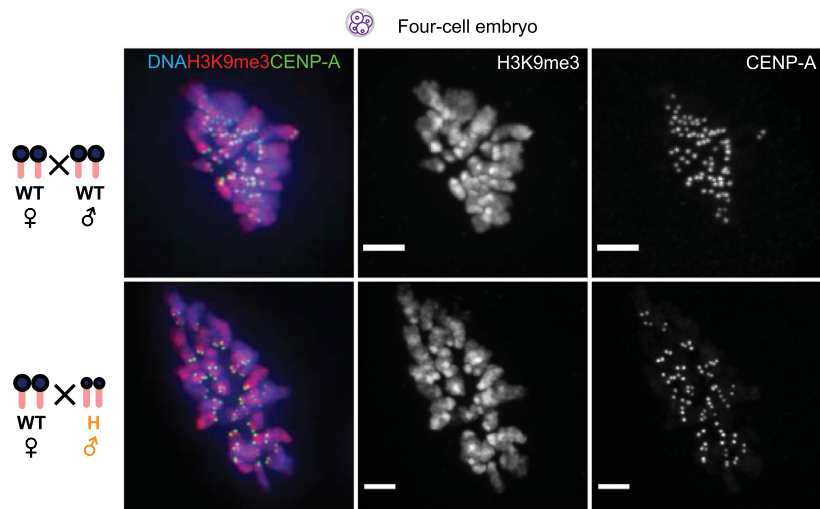
## Prediction from model:

Epigenetic differences in zygote should equalize by four cell stage. (Tested in Fig. 6a)

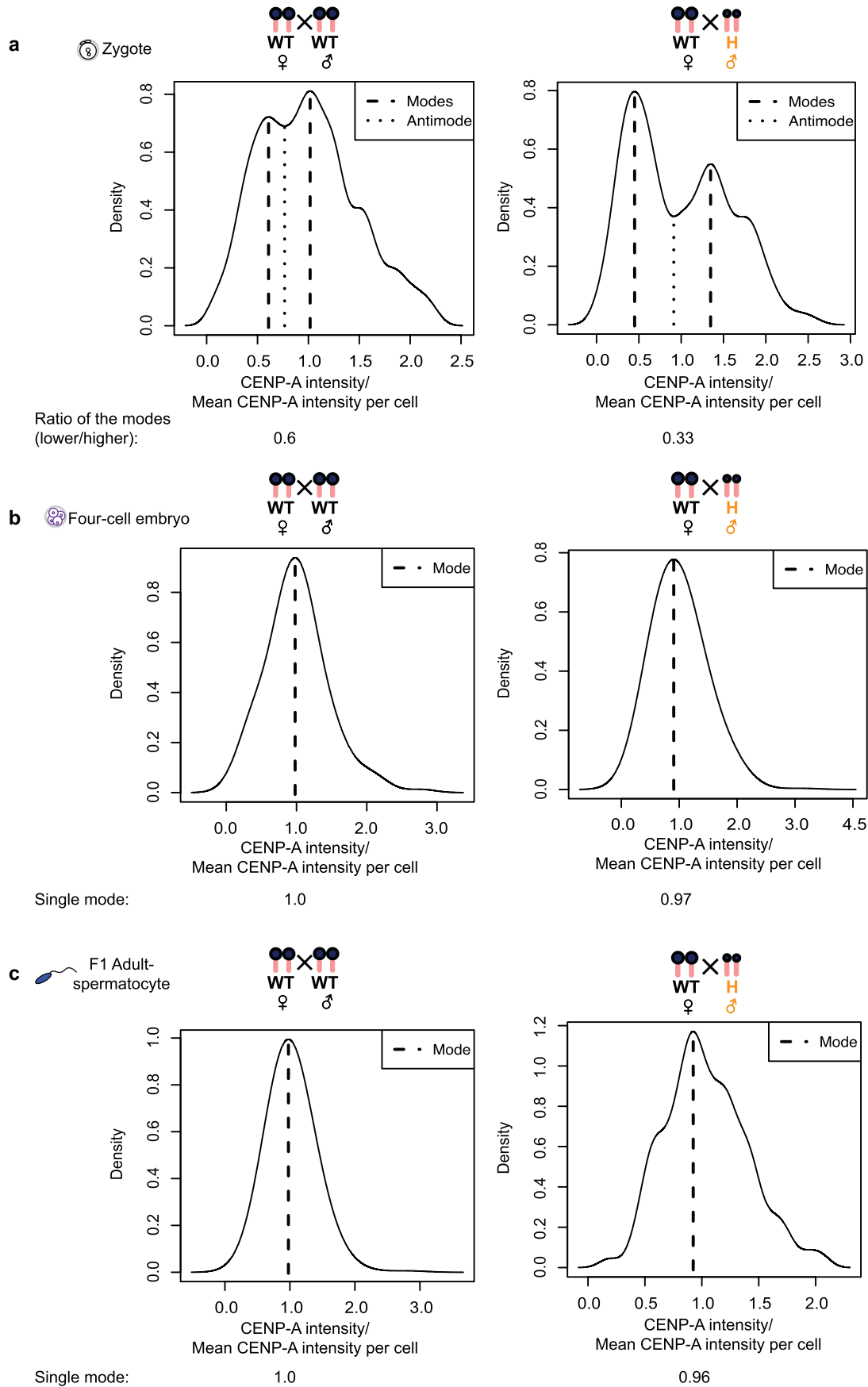
**Extended Data Fig. 5 | Model to explain equalization of epigenetic differences and subsequent memory.** **a**, Assumptions used for the modelling. **b**, Epigenetic inheritance of CENP-A as determined in cycling somatic cells in culture by replication coupled dilution and G1 reloading. **c**, Example calculation and graph for CENP-A assembly in the first two embryonic cell cycles for progeny of a WT x WT cross. For simplicity, initial CENP-A levels are set to 100 and 50 on the maternal and paternal centromeres, respectively, based on our measurements in zygotes (Fig. 3c). At each S-phase, CENP-A levels are diluted by half on each centromere, and we assume equal assembly on maternal and paternal centromeres in the following G1. Assembly in the first cell cycle depends on the maternal pool, set to 100 for a zygote from a WT female, giving an increase of 50 on both maternal and paternal centromeres. Assembly in the second cell cycle depends on the zygotic pool, which is set to 100 for a WT zygotic genotype. **d**, Graphs from similar calculations as b, for the designated crosses. Initial CENP-A levels are set to 50 for maternal centromeres from *Cenpa*<sup>+/-</sup> mothers and 40 for paternal centromeres from *Cenpa*<sup>+/-</sup> fathers, based on our measurements (Fig. 1c and Fig. 3c). Arrows indicate equal assembly on maternal and paternal centromeres. In the first cell cycle, assembly is from a maternal pool of 100 (black arrows) or 50 (yellow arrows) for WT or *Cenpa*<sup>+/-</sup> mothers, respectively. In the second cell cycle, assembly is from a zygotic pool of 100 (purple arrows), reflecting a WT zygotic genotype. Calculations show equalization by the four-cell stage in all crosses. Furthermore, crosses with reduced maternal contribution (H♀) equalize to a lower level, which is then remembered through development. Source numerical data are available in source data.



**Extended Data Fig. 6 | 3' UTR of *Cenpa* message has hallmarks of dormant maternal mRNA. a**, Polyadenylation (addition of a poly (A) tail) of mRNA is a mechanism to control gene expression. Nuclear polyadenylation is an essential part of post-transcriptional processing of most mRNAs, dictated by the ubiquitous cis-element 3' UTR hexameric motif AATAAA (nuclear polyadenylation element, NPE). Dormant maternal mRNAs are deposited in the oocyte with short poly(A) tails and are translationally inactive. After fertilization, these maternal mRNAs undergo translation by elongation of the poly(A) tail, controlled by a cytoplasmic polyadenylation element (CPE) usually present within 100 nt upstream of the NPE<sup>28</sup>. We find conserved CPEs in the mouse, human and frog *Cenpa* 3' UTRs (CPE I = TTTTAT or CPE II = TTTTAA) upstream of the NPE as expected for dormant maternal mRNAs. **b**, Analysis of 12 sequenced rodent species<sup>38</sup> reveals that CPEs (CPE I in bold boxes and CPE II in dashed boxes) are present upstream of the NPE in every species as expected for a maternal effect gene.

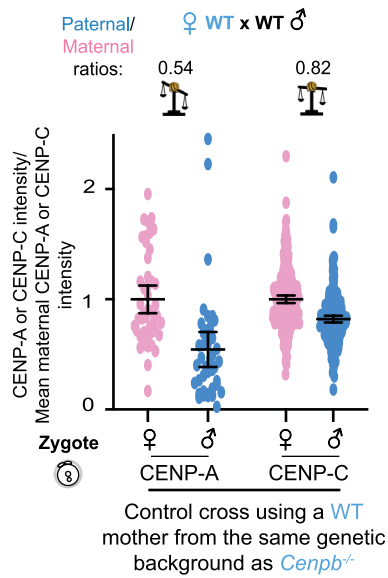


**Extended Data Fig. 7 | Symmetric distribution of H3K9me3 at the four-cell stage.** Representative cell from four-cell embryos for each of the two denoted crosses with H3K9me3 (red), CENP-A (green) and DNA (blue). H3K9me3 is present on both maternal and paternal chromatin at this stage, in contrast to zygotes (Fig. 3b and Fig. 6b–e). Scale bars: 5  $\mu$ m.



Extended Data Fig. 8 | See next page for caption.

**Extended Data Fig. 8 | CENP-A intensity distribution changes from bimodal to unimodal in early embryogenesis.** Graphs show locations of the modes in each distribution from Fig. 6a. **a**, The WT x WT and WT♀ x H♂ zygote distributions contain two modes (dashed lines) on either side of a central antimode (dip, pointed lines) characteristic of bimodal distributions<sup>52</sup>. The separation between the two modes is greater in the WT♀ x H♂ cross as expected. In addition, the ratios of the values of the two modes (x-axis) denoted under each cross agree well with the ratios of paternal to maternal centromere intensities calculated in Figs. 3c and 6f. **b,c**, Similar plots of four-cell embryos (b) from the same crosses show a single central mode characteristic of a unimodal population, like the F1 adult spermatocytes (c), which represents a uniform centromere population. The ratio of the modes in bimodal or the value of the mode in unimodal distribution is indicated below the graphs. Source numerical data are available in source data.



**Extended Data Fig. 9 | Genetic pathway for centromere equalization. a.** Quantifications of maternal (pink) and paternal (blue) CENP-A and CENP-C intensities in zygotes from a WT x WT control for the *Cenpb*<sup>-/-</sup> strain<sup>38</sup>, with average paternal/maternal CENP-A or CENP-C ratios above; N = 46, 42, 237, 231 centromeres (left to right). Error bars: median ± 95% CI. Although these animals are in a CF-1/C57BL/6J/DBA/2J background, CENP-A and CENP-C ratios in WT zygotes using mothers from this background are consistent with those of C57BL/6J alone (Fig. 6b,f). Source numerical data are available in source data.

## Reporting Summary

Nature Portfolio wishes to improve the reproducibility of the work that we publish. This form provides structure for consistency and transparency in reporting. For further information on Nature Portfolio policies, see our [Editorial Policies](#) and the [Editorial Policy Checklist](#).

### Statistics

For all statistical analyses, confirm that the following items are present in the figure legend, table legend, main text, or Methods section.

n/a Confirmed

- |                                     |                                     |  |
|-------------------------------------|-------------------------------------|--|
| <input type="checkbox"/>            | <input checked="" type="checkbox"/> | The exact sample size ( $n$ ) for each experimental group/condition, given as a discrete number and unit of measurement  |
| <input type="checkbox"/>            | <input checked="" type="checkbox"/> | A statement on whether measurements were taken from distinct samples or whether the same sample was measured repeatedly  |
| <input type="checkbox"/>            | <input checked="" type="checkbox"/> | The statistical test(s) used AND whether they are one- or two-sided<br><i>Only common tests should be described solely by name; describe more complex techniques in the Methods section.</i>   |
| <input checked="" type="checkbox"/> | <input type="checkbox"/>            | A description of all covariates tested   |
| <input type="checkbox"/>            | <input checked="" type="checkbox"/> | A description of any assumptions or corrections, such as tests of normality and adjustment for multiple comparisons  |
| <input type="checkbox"/>            | <input checked="" type="checkbox"/> | A full description of the statistical parameters including central tendency (e.g. means) or other basic estimates (e.g. regression coefficient) AND variation (e.g. standard deviation) or associated estimates of uncertainty (e.g. confidence intervals) |
| <input type="checkbox"/>            | <input checked="" type="checkbox"/> | For null hypothesis testing, the test statistic (e.g. $F$ , $t$ , $r$ ) with confidence intervals, effect sizes, degrees of freedom and $P$ value noted<br><i>Give <math>P</math> values as exact values whenever suitable.</i>                            |
| <input checked="" type="checkbox"/> | <input type="checkbox"/>            | For Bayesian analysis, information on the choice of priors and Markov chain Monte Carlo settings   |
| <input checked="" type="checkbox"/> | <input type="checkbox"/>            | For hierarchical and complex designs, identification of the appropriate level for tests and full reporting of outcomes   |
| <input checked="" type="checkbox"/> | <input type="checkbox"/>            | Estimates of effect sizes (e.g. Cohen's $d$ , Pearson's $r$ ), indicating how they were calculated   |

*Our web collection on [statistics for biologists](#) contains articles on many of the points above.*

### Software and code

Policy information about [availability of computer code](#)

Data collection Data collection: Metamorph (Molecular devices, v7.10.3.294) for image acquisition

Data analysis Statistical analyses were performed with Prism (GraphPad Software Inc., versions 7.0e, 8.4.3 & 9.0.0) and R (open source, <https://www.rproject.org>); images were analyzed with Fiji/ImageJ (open source at <https://imagej.net/>, version 2.1.0/1.53c). MAFFT version 7 and Unipro Version 37 was used for multiple sequence alignment.

For manuscripts utilizing custom algorithms or software that are central to the research but not yet described in published literature, software must be made available to editors and reviewers. We strongly encourage code deposition in a community repository (e.g. GitHub). See the Nature Portfolio [guidelines for submitting code & software](#) for further information.

### Data

Policy information about [availability of data](#)

All manuscripts must include a [data availability statement](#). This statement should provide the following information, where applicable:

- Accession codes, unique identifiers, or web links for publicly available datasets
- A description of any restrictions on data availability
- For clinical datasets or third party data, please ensure that the statement adheres to our [policy](#)

Previously published microarray data for long poly-(A) tailed Cenpa mRNA in pre-implantation development is available freely on NCBI Gene Expression Omnibus (GEO) database (Accession no: GDS813 from reference series: GSE1749). The 12 mouse genomes used for Cenpa 3'UTR analysis are available at NCBI BioProject database (<https://www.ncbi.nlm.nih.gov/bioproject>) under accession number PRJNA669840. Source data have been provided in Source Data. All other data supporting the findings of this study are available from the corresponding author on reasonable request.

## Field-specific reporting

Please select the one below that is the best fit for your research. If you are not sure, read the appropriate sections before making your selection.

Life sciences       Behavioural & social sciences       Ecological, evolutionary & environmental sciences

For a reference copy of the document with all sections, see [nature.com/documents/nr-reporting-summary-flat.pdf](https://www.nature.com/documents/nr-reporting-summary-flat.pdf)

## Life sciences study design

All studies must disclose on these points even when the disclosure is negative.

Sample size	No statistical method was used to determine sample sizes. Sample sizes for all experiments were determined by the current standard used for mouse model systems in epigenetic experiments, based on the minimal amount of mice required to detect significance with an alpha rate set at .05 in a standardly powered experiment. The number of animals and replicates were determined based on the consistency of the phenotype. In most cases, the phenotype was consistent and penetrant as is obvious from the agreement between multiple independent replicates, validating the sample size is sufficient.
Data exclusions	No data were excluded from analysis.
Replication	All experiments have 2-5 replicates with multiple animals in each totaling at least 4-8 per experiment per genotype. The animals in each generation were produced from multiple mating pairs. For IVF and embryo collections, at least 3 replicates were performed each having at least 5 females mated to male(s) (5-8 for in vivo fertilization and 1 for in vitro fertilization). Importantly, most replicates showed similar trends and all the data is presented in the paper and in source data files. Also, we confirmed that in vivo and in vitro fertilized embryos show similar ratios (each method repeated 2-3 times) validating our results further. Lastly, all the conclusions in this study are drawn from multiple animals sampled from many litters from different mating pairs for each generation. Detailed replicate numbers for all figures are provided in the Supplementary Table 1 and source data files.
Randomization	Randomization is built into our experiments as each animal was chosen from a different litter and mating pair, no data was excluded and all cells were imaged at random. Samples are designated as control or experiment according to their genotyping data. Animals were genotyped twice. Within a genotype animals are randomly picked. Since our experiment is with a heterozygous single deletion within the genome, we do not have any covariates to consider.
Blinding	Investigators were not blinded for data collection (imaging) and quantifications (data analysis) as the phenotype automatically reports on the genotype consistently and is very penetrant. Likewise, statistical analysis of bimodality did not require blinding since the rotated kernel density (violin) plots being analyzed show obvious bi/uni-modality in each cross. Blinding in cases of an obvious phenotype is unnecessary.

## Reporting for specific materials, systems and methods

We require information from authors about some types of materials, experimental systems and methods used in many studies. Here, indicate whether each material, system or method listed is relevant to your study. If you are not sure if a list item applies to your research, read the appropriate section before selecting a response.

### Materials & experimental systems

n/a	Involved in the study
<input type="checkbox"/>	<input checked="" type="checkbox"/> Antibodies
<input checked="" type="checkbox"/>	<input type="checkbox"/> Eukaryotic cell lines
<input checked="" type="checkbox"/>	<input type="checkbox"/> Palaeontology and archaeology
<input type="checkbox"/>	<input checked="" type="checkbox"/> Animals and other organisms
<input checked="" type="checkbox"/>	<input type="checkbox"/> Human research participants
<input checked="" type="checkbox"/>	<input type="checkbox"/> Clinical data
<input checked="" type="checkbox"/>	<input type="checkbox"/> Dual use research of concern

### Methods

n/a	Involved in the study
<input checked="" type="checkbox"/>	<input type="checkbox"/> ChIP-seq
<input checked="" type="checkbox"/>	<input type="checkbox"/> Flow cytometry
<input checked="" type="checkbox"/>	<input type="checkbox"/> MRI-based neuroimaging

## Antibodies

### Antibodies used

Primary antibodies used are as follows:

- Rabbit anti-mouse CENP-A: Cell Signaling, 2048S, C51A7,4, 1:200 (oocytes, embryos, bone marrow), 1:400 (spermatocytes)
- Mouse anti-mouse H3K9me3: Active motif, 39285, 2AG-6F12-H4, 03019002, 1:500 (embryos)
- Rabbit anti-mouse CENP-C (this study, details are in Methods), 1:1000 in embryos.

Secondary antibodies used are:

- Donkey anti-rabbit Alexa Fluor 488: Invitrogen, A21206, 1113537 1:500 (oocytes, embryos, bone marrow), 1:2000 (spermatocyte spreads)
- Donkey anti-mouse Alexa Fluor 594: Invitrogen, A11032, 1: 500
- Mouse anti-mouse SYCP3: Abcam, ab97672, 10G11/7, 1:200

## Validation

All the antibodies used are commercially available except for anti-mouse CENP-C and are validated for use in immunocytochemistry. Validation information is provided in the links below:  
 Rabbit anti-mouse CENP-A: Cell Signaling, 2048S, C51A7, see manufacturer's website for references and validation information (<https://www.cellsignal.com/products/primary-antibodies/cenp-ac51a7-rabbit-mab-mouse-specific/2048>)  
 -Mouse anti-mouse H3K9me3: Active motif, 39285, 2AG-6F12-H4, 03019002, see manufacturer's website for references and validation (<https://www.activemotif.com/catalog/details/39285/histone-h3-trimethyl-lys9-antibody-mabclone-2ag-6f12-h4>)  
 -Rabbit anti-mouse CENP-C (this study, details are in Methods). The rabbit anti-mouse CENP-C was validated for this study through both Western blot and immunocytochemistry on NIH3T3 cells (reactivity) and human cell lysates (no reactivity). The antibody recognizes a band at the expected molecular weight of ~130kDa by immunoblot. It recognizes punctate centromeric foci in both NIH3T3 cells and mouse embryos (1:1000 dilution).

Secondary antibodies used are:

-Donkey anti-rabbit Alexa Fluor 488: Invitrogen, A21206, 1113537, see manufacturer's website for references and validation (<https://www.thermofisher.com/antibody/product/Donkey-anti-Rabbit-IgG-H-L-Highly-Cross-Adsorbed-Secondary-Antibody-Polyclonal/A-21206>)  
 -Donkey anti-mouse Alexa Fluor 594: Invitrogen, A11032, see manufacturer's website for references and validation (<https://www.thermofisher.com/antibody/product/Goat-anti-Mouse-IgG-H-L-Highly-Cross-Adsorbed-Secondary-Antibody-Polyclonal/A-11032>)  
 -Mouse anti-mouse SYCP3: Abcam, ab97672, 10G11/7, see manufacturer's website for references and validation (<https://www.abcam.com/scp3-antibody-cor-10g117-ab97672.html>)

## Animals and other organisms

Policy information about [studies involving animals](#); [ARRIVE guidelines](#) recommended for reporting animal research

### Laboratory animals

Mouse strains used in this study are as follows:

-Cenpa<sup>Fl/Fl</sup>;Gdf9<sup>Cre/+</sup> females (described in reference 28)  
 -Cenpa<sup>+/-</sup> heterozygous males and females (this study, see Methods)  
 -C57BL6/J males and females (Jackson Laboratory, 000664),  
 -ZALENDE/Eij (CHPO) males (Jackson laboratory, 001392)  
 -Cenpb<sup>-/-</sup> knockout females (described and validated in reference 38)

All data was collected from animals that were reproductively mature (at least 6-8 weeks of age) and less than 6-month-old. Both male and female animals were used wherever possible.

Mouse colony breeding conditions:

Light/dark cycle: 12 hours each

Bred at room temperature with minimal disturbance with a range of 30-70% humidity depending on the season.

All animal experiments and protocols were approved by the Institutional Animal Use and Care Committee of the University of Pennsylvania and were consistent with National Institutes of Health guidelines (protocol #803994)

### Wild animals

No wild animals were used in this study.

### Field-collected samples

There were no field samples in this study.

### Ethics oversight

All protocols were overseen by Institutional Animal Use and Care Committee of the University of Pennsylvania.

Note that full information on the approval of the study protocol must also be provided in the manuscript.